

Emulation-based Neuromorphic Control for the Stabilization of LTI Systems

Elena Petri, Koen J.A. Scheres, Erik Steur, and W.P.M.H. (Maurice) Heemels

Abstract—Brain-inspired neuromorphic technologies can offer important advantages over classical digital clock-based technologies in various domains, including systems and control engineering. Indeed, neuromorphic engineering could provide low-latency, low-energy and adaptive control systems in the form of spiking neural networks (SNNs) exploiting spike-based control and communication. However, systematic methods for designing and analyzing neuron-inspired spiking controllers are currently lacking. This paper presents a new systematic approach for stabilizing linear time-invariant (LTI) systems using SNN-based controllers, designed as a network of integrate-and-fire neurons, whose input is the measured output from the plant and generating spiking control signals. The new approach consists of a two-step emulation-based design procedure. In the first step, we establish conditions on the neuron parameters to ensure that the spiking signal generated by a pair of neurons emulates any continuous-time signal input to the neurons with arbitrary accuracy in terms of a special metric for spiky signals. In the second step, we propose a novel stability notion, called integral spiking-input-to-state stability (iSISs) building on this special metric. We prove that an asymptotically stable LTI system has this iSISs property. By combining these steps, a certifiable practical stability property of the closed-loop system can be established. Generalizations are discussed and the effectiveness of the approach is illustrated in a numerical case study.

Index Terms—Neuromorphic control, stability analysis, spiking neural networks, input-to-state stability

I. INTRODUCTION

Many potential advantages of asynchronous and event-driven brain-inspired technologies over classical digital clock-based technologies, including energy efficiency, adaptability and robustness [1], have motivated numerous research activities in various engineering fields in recent years, see e.g., [2]–[6] and the references therein. This trend is also witnessed in the systems and control community, where neuromorphic control is an emerging research topic, aiming at designing controllers whose dynamics is inspired by biological neurons in the brain. In fact, the potential of brain-inspired control was first illustrated more than thirty years ago in experimental studies in [7], [8] for the regulation of the speed of an electric motor. Recent works have addressed the challenge of designing neuron-inspired controllers, see, e.g., [9]–[17]

Elena Petri, Erik Steur and Maurice Heemels are with the Department of Mechanical Engineering, Eindhoven University of Technology, The Netherlands. {e.petri, e.steur, m.heemels}@tue.nl

Koen Scheres is with the Department of Electrical Engineering (ESAT), STADIUS, KU Leuven, Leuven 3001, Belgium. koen.scheres@kuleuven.be

and the references therein. Despite these interesting contributions, a key fundamental open problem from a control theory perspective is the creation of a formal framework for the modeling, design and analysis of spiking neuromorphic controllers.

A natural way to model neuromorphic control systems is through spiking neural networks (SNNs). Modeling spiking controllers as neuronal networks, naturally connects this line of research to the literature of neural network-based control, where artificial neural networks (ANNs) have been widely studied, see, e.g., [18]–[20]. Unlike ANNs, SNNs operate through event-based asynchronous spikes, and therefore more closely mimic biological neuronal dynamics with the potential to provide the promising advantages of brain-inspired technologies. However, the event-based-spiking nature also introduces crucial theoretical challenges for their analysis and design.

The goal of this work is to address these challenges by contributing towards a mathematically rigorous analysis and design framework for spiking neuromorphic controllers for LTI systems (and beyond). To stress, our objective is not to illustrate improvements in terms of energy-efficiency, robustness and/or adaptability compared to existing non-spiking control techniques, although we comment upon this briefly in Remark 5 below, but we aim to provide a systematic approach to design and analyze neuromorphic controllers ensuring important closed-loop stability guarantees. In our previous work [21], we already proved a practical stability property of a spiking controller, based on the leaky integrate-and-fire neuronal model, interconnected with a *first-order* linear time-invariant (LTI) system. The assumption of first-order plant dynamics was crucial in [21], as the proof relied on the explicit solution of the controlled system between spikes and on the knowledge of the direction of the spiking control input, making generalization to higher-dimensional systems virtually impossible. In this paper, we therefore follow a completely different approach, which, as we will show, applies naturally to higher-order and multi-input multi-output (MIMO) systems.

The approach followed in this work is based on *emulation-based* design of neuromorphic controllers that practically stabilize LTI plants, in which the SNN-based dynamics of the controllers is inspired by the integrate-and-fire neuronal model [22]–[24], [25, Chapter 4]. To not blur the main conceptual ideas by too many technicalities, we first focus on a single-input single-output (SISO) LTI system (of any order), assumed to be stabilizable via static output feedback. Later in the paper we will extend this approach to MIMO systems and other types

of controllers. The proposed emulation-based design approach consists of two steps. In *the first step*, we provide conditions on the neuron's parameters (i.e., the spike's amplitude and the firing threshold) such that the spiking control signal generated by the neuromorphic controller approximates the “positive part of the input signal”, i.e., the time-function $t \mapsto \max(0, y(t))$ (reminding of the famous RELU functions used in ANNs), in an appropriate sense, where y represents the continuous-time input signal to the neuron. This result is closely related to the well-known *universal approximation property*, see, e.g., [26], [27], where static nonlinear mappings can be arbitrarily closely approximated by ANNs on compact domains. However, our result is different in the sense that we demonstrate that the error between the positive part of the input signal and the spiky output signal of the neuron can be made arbitrarily small in an *integral sense* by tuning the neuron's parameters. We will demonstrate that any piecewise affine (PWA) continuous mapping can be approximated (“emulated”) by a network of integrate-and-fire neurons on the signal level in an integral sense. This formal signal-based approximation property of integrate-and-fire neurons forms our first main contribution and is crucial to our emulation approach.

The second step of the emulation-based design approach consists in guaranteeing a new stability notion, for which we coin the name *integral Spiking-Input-to-State Stability* (iSISS). This property allows to consider spiking input signals, and, in some cases, it is a stronger property than the existing notion of integral input-to-state stability in [28], [29]. The second contribution of this work is the definition of this new stability concept, as well as the proof that an asymptotically stable LTI system is iSISS with respect to spiking inputs. Interestingly, this result relies on an integration-by-parts method for irregular signals containing spikes modeled as Dirac pulses. We believe that the iSISS property plays an instrumental role for guaranteeing stability properties for (nonlinear) systems controlled by spiking signals. This work is the first to define this property and to reveal its important role in this context.

By combining the iSISS property with the “spiky signal-based universal approximation property,” we ensure that the trajectory of the LTI system in closed loop with a spiking controller emulates the continuous-time trajectory we would have obtained if a stabilizing static output feedback controller would have been used, in the sense that we provide a tunable bound on the difference between the two trajectories for all times. As a consequence, a practical stability property of the LTI system in closed loop with the spiking controller can be established, which forms our third main contribution.

As previously said, for ease of exposition and to keep focus on the core concepts and reasoning, we first develop our result for SISO LTI systems. We then explain how the neuronal network and the obtained signal-based universal approximation property and stability results are generalizable to multiple-input multiple-output (MIMO) LTI systems.

Compared to the preliminary conference version of this work [30], several results are generalized and proofs are now provided. In particular, we present the spiky signal-based universal approximation property for each neuron separately, and not only for a two-neuron controller approximating a

linear scalar function, and we now also consider networks of spiky neurons with more than two neurons, emulating continuous PWA functions. Compared to [30], more insights and properties of the iSISS property are given, and the stability result is generalized to MIMO LTI systems. An additional property ensured in this paper is that no accumulation of spiking times can happen, and thus the Zeno phenomenon cannot occur. Finally, a new numerical example is presented.

The remainder of the paper is organized as follows. Preliminaries are reported in Section II and the system setup and the two-neuron spiking controller for SISO LTI systems are presented in Section III. The emulation-based design approach is described in Section IV and the signal-based universal approximation property of spiking neuronal networks is established in Section V. Section VI presents the notion of iSISS, which is then used in Section VII to guarantee a practical stability property of the SISO LTI system in closed loop with the two-neuron spiking controller. Generalizations to MIMO LTI systems and the approximation of PWA functions are described in Section VIII, and a numerical example illustrates the results in Section IX. Finally, Section X concludes the paper and presents possible future work directions. Proofs and a technical lemma are given in the Appendix.

II. PRELIMINARIES

The notation \mathbb{R} stands for the set of real numbers, $\mathbb{R}_{\geq 0} := [0, +\infty)$ and $\mathbb{R}_{>0} := (0, +\infty)$. We use \mathbb{Z} to denote the set of integers, $\mathbb{Z}_{\geq 0} := \{0, 1, 2, \dots\}$ and $\mathbb{Z}_{>0} := \{1, 2, \dots\}$. Given a function $f : \mathbb{R}_{\geq 0} \rightarrow \mathbb{R}$, for any $t \geq 0$ we denote by $f(t^+)$ the right limit of f at t , i.e., $f(t^+) = \lim_{s \downarrow t} f(s)$, and with $f(t^-)$ the left limit, i.e., $f(t^-) = \lim_{s \uparrow t} f(s)$. For a vector $x \in \mathbb{R}^n$, $|x|$ denotes its Euclidean norm. For a matrix $A \in \mathbb{R}^{n \times m}$, $\|A\|$ stands for its induced 2-norm. For a Lebesgue measurable signal $v : \mathbb{R}_{\geq 0} \rightarrow \mathbb{R}^{n_v}$ with $n_v \in \mathbb{Z}_{>0}$, and $t_1, t_2 \in \mathbb{R}_{\geq 0} \cup \{\infty\}$ with $t_1 \leq t_2$, $\|v\|_{[t_1, t_2]} := \text{ess. sup}_{t \in [t_1, t_2]} |v(t)|$. A continuous function $\alpha : [0, a) \rightarrow [0, \infty)$ is of class \mathcal{K} , if $\alpha(0) = 0$ and α is strictly increasing. Moreover, α is of class \mathcal{K}_∞ if, additionally, $a = \infty$ and $\lim_{r \rightarrow \infty} \alpha(r) = \infty$. A continuous function $\beta : [0, \infty) \times [0, \infty) \rightarrow [0, \infty)$ is of class \mathcal{KL} if, for any fixed $s \in \mathbb{R}_{\geq 0}$, $\beta(\cdot, s) \in \mathcal{K}$ and, for each fixed $r \in \mathbb{R}_{\geq 0}$, $\beta(r, \cdot)$ is non-increasing and satisfies $\lim_{s \rightarrow \infty} \beta(r, s) = 0$. Given a set $\mathcal{Y} \subseteq \mathbb{R}^{n_y}$ with $n_y \in \mathbb{Z}_{>0}$, $\mathcal{L}_{\mathcal{Y}}$ denotes the set of all functions y from $\mathbb{R}_{\geq 0}$ to \mathcal{Y} that are Lebesgue measurable and locally essentially bounded. By δ , we denote the Dirac delta function (distribution), which is defined as $\delta(t) = 0$ when $t \neq 0$, $\delta(t) = +\infty$ when $t = 0$ and it is such that $\int_{-\infty}^{+\infty} \delta(t) dt = 1$. We use sign for the set-valued map sign: $\mathbb{R} \rightrightarrows \{-1, 1\}$ defined as, for any $z \in \mathbb{R}$, $\text{sign}(z) = \{1\}$ if $z > 0$, $\text{sign}(0) = \{-1, 1\}$ and $\text{sign}(z) = \{-1\}$ if $z < 0$.

III. SYSTEM AND NEUROMORPHIC CONTROLLER

Consider the control of a linear time-invariant (LTI) system, given by

$$\dot{x} = Ax + Bu, \quad y = Cx, \quad (1)$$

where $x \in \mathbb{R}^{n_x}$ is the state, with $x(0) = x_0 \in \mathbb{R}^{n_x}$, $y \in \mathbb{R}^{n_y}$ is the output and $u \in \mathbb{R}^{n_u}$ is the (spiking) control input and $n_x, n_y, n_u \in \mathbb{Z}_{>0}$. We start from the next assumption.

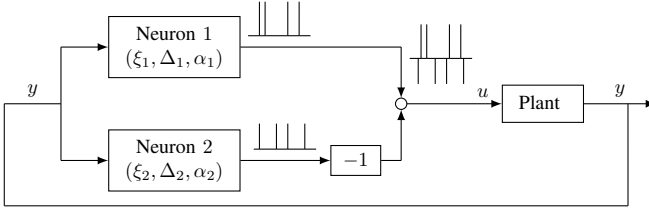


Fig. 1. Block diagram representing the system architecture for a SISO setup.

Assumption 1. There exists $K \in \mathbb{R}^{n_y \times n_u}$ such that the matrix $A + BKC$ is Hurwitz, with $A \in \mathbb{R}^{n_x \times n_x}$, $B \in \mathbb{R}^{n_x \times n_u}$ and $C \in \mathbb{R}^{n_y \times n_x}$ from (1).

A sufficient and necessary condition to satisfy Assumption 1 can be found in, e.g., [31, Theorem 5]. Our goal is to design a neuromorphic controller generating a spiking control signal $u \in \mathbb{R}^{n_u}$ such that the closed-loop system emulates, in a sense that will be clarified below, the asymptotically stable closed loop, corresponding to $\dot{x} = (A+BKC)x$, from Assumption 1. For ease of exposition we first consider single-input single-output (SISO) LTI systems, namely (1) with $n_u = n_y = 1$. In Section VIII-A we will generalize the results to multiple-input multiple-output (MIMO) LTI systems.

We consider the control configuration shown in Fig. 1, where the spiking input u is generated by a neuromorphic controller consisting of two neurons, whose dynamics is inspired by the integrate-and-fire neuron model [22]–[24], [25, Chapter 4]. In particular, $\xi_\ell \in \mathbb{R}_{\geq 0}$, $\ell \in \{1, 2\}$, represents the membrane potential of the neuron, whose continuous-time dynamics is a first-order differential equation affected by a continuous and nonnegative (current) input, and it is then reset whenever it reaches a positive threshold. The choice of the integrate-and-fire neuronal model has been made because it is a simple, yet insightful mathematical model of neuronal dynamics and it allows us to study properties of systems in closed loop with spiking controllers. Moreover, this neuronal model is a well-known and well-accepted model for describing neuronal dynamics and can be implemented with electrical circuits, see, e.g., [32]–[35]. Although neurons can be sensitive to negative inputs via the so-called rebound spiking mechanism [36], in this work we only consider the integrate-and-fire neuron model, which as explained in [25], generates spiking times only when fed with nonnegative inputs. As such, the input to each of the neurons is taken as a signed version of the continuous-time measured output y of system (1) with $n_y = 1$, which, depending on its sign, influences either ξ_1 or ξ_2 , in our neuromorphic control setup. This leads to one neuron being sensitive to positive values of y , through $\max\{0, y\}$, and one to negative values of y , through $\max\{0, -y\}$. We thus consider the following dynamics between two spiking actions,

$$\frac{d}{dt}\xi_1(t) = \max\{0, y(t)\}, \quad t \in [t_{1,j_1}, t_{1,j_1+1}), j_1 \in \mathbb{Z}_{\geq 0}, \quad (2a)$$

$$\frac{d}{dt}\xi_2(t) = \max\{0, -y(t)\}, \quad t \in [t_{2,j_2}, t_{2,j_2+1}), j_2 \in \mathbb{Z}_{\geq 0}, \quad (2b)$$

where $t_{1,0} = t_{2,0} = 0$ and $\xi_\ell(0) \in [0, \Delta_\ell]$, where $\Delta_\ell \in \mathbb{R}_{>0}$

is the firing threshold, which is a neuron parameter, and the sequence $\{t_{\ell,j_\ell}\}_{j_\ell \in \mathbb{Z}_{\geq 0}}$ represents the spiking instants of ξ_ℓ , $\ell \in \{1, 2\}$. Moreover, for any $t \in \mathbb{R}_{\geq 0}$, $j_\ell(t) \in \mathbb{Z}_{\geq 0}$ counts the number of spikes generated by neuron ℓ up to, and including, time $t \in \mathbb{R}_{\geq 0}$. Neuron $\ell \in \{1, 2\}$, generates spikes when

$$\xi_\ell \geq \Delta_\ell \quad (3)$$

is satisfied. The sequence $\{t_{\ell,j_\ell}\}_{j_\ell \in \mathbb{Z}_{\geq 0}}$, $\ell \in \{1, 2\}$, is therefore defined as

$$t_{\ell,0} = 0, \quad t_{\ell,j_\ell+1} := \inf\{t > t_{\ell,j_\ell} : \xi_\ell(t) \geq \Delta_\ell\}. \quad (4)$$

Note that, according to (4), $t_{\ell,0} = 0$ is not a spiking time of neuron $\ell \in \{1, 2\}$, and the first spiking time is $t_{\ell,1} \in \mathbb{R}_{>0}$. The sequence of spiking times of the two-neuron network is given by $\{t_j\}_{j \in \mathbb{Z}_{\geq 0}} := \{t_{1,j_1}\}_{j_1 \in \mathbb{Z}_{\geq 0}} \cup \{t_{2,j_2}\}_{j_2 \in \mathbb{Z}_{\geq 0}}$, where, similarly to (4), $t_0 = t_{1,0} = t_{2,0} = 0$ is not a spiking time.

Inspired by the integrate-and-fire neuron model, where the membrane potential of the neuron is reset whenever it reaches a threshold, we reset the variable ξ_ℓ , $\ell \in \{1, 2\}$, when it generates a spike, while it is not modified when the other neuron reaches the threshold, i.e., when neuron $\ell \in \{1, 2\}$ satisfies (3) at time t_{ℓ,j_ℓ} , $j_\ell \in \mathbb{Z}_{\geq 0}$, and thus is the firing neuron,

$$\xi_\ell(t_{\ell,j_\ell}^+) = 0, \quad \xi_{3-\ell}(t_{\ell,j_\ell}^+) = \xi_{3-\ell}(t_{\ell,j_\ell}). \quad (5)$$

It is important to notice that the integrate-and-fire neuron model does not include a spike generation mechanism, but, as explained in [24], it is only a threshold mechanism and therefore does not intrinsically produce a spike. In our design, we add a spike generation mechanism to the integrate-and-fire neuron model. Indeed, whenever ξ_ℓ , $\ell \in \{1, 2\}$, reaches the threshold Δ_ℓ , a spiking control action, is fired, whose sign depends on which neuron reaches Δ_ℓ . Note that hardware implementations of neuromorphic controllers in the literature, see, e.g., [11], [13], [14], [16], produce spiking signals. In particular, when ξ_1 reaches the threshold, the resulting spiking control action at the spiking time t_{1,j_1} , $j_1 \in \mathbb{Z}_{\geq 0}$, is given by $+\alpha_1 \delta(t - t_{1,j_1})$, with $\alpha_1 \in \mathbb{R}_{>0}$ the amplitude of the spiking control action applied to the plant and $t \in \mathbb{R}_{\geq 0}$. Similarly, when ξ_2 reaches the threshold, the resulting spiking control action at the spiking time t_{2,j_2} , $j_2 \in \mathbb{Z}_{\geq 0}$, is given by $-\alpha_2 \delta(t - t_{2,j_2})$, with $\alpha_2 \in \mathbb{R}_{>0}$ and $t \in \mathbb{R}_{\geq 0}$. In the following, with some abuse of terminology, we consider $\alpha_\ell \in \mathbb{R}_{>0}$, $\ell \in \{1, 2\}$, a neuron parameter.

We now define the spiking input generated by each neuron as, for each $\ell \in \{1, 2\}$, and all $t \in \mathbb{R}_{\geq 0}$,

$$u_\ell(t) = \sum_{i=1}^{+\infty} (3 - 2\ell) \alpha_\ell \delta(t - t_{\ell,i}). \quad (6)$$

Note that $(3 - 2\ell) = 1$, when $\ell = 1$ and $(3 - 2\ell) = -1$ when $\ell = 2$. Therefore, $(3 - 2\ell)$ simply considers the sign of the spiking output of the neuron. Using (6), we define the spiking signal u generated by the two integrate-and-fire neurons in the parallel configuration in Fig. 1 as, for all $t \in \mathbb{R}_{\geq 0}$,

$$\begin{aligned} u(t) &= u_1(t) + u_2(t) \\ &= \sum_{i=1}^{+\infty} \alpha_1 \delta(t - t_{1,i}) + \sum_{i=1}^{+\infty} -\alpha_2 \delta(t - t_{2,i}). \end{aligned} \quad (7)$$

Defining solutions to general (nonlinear) systems with spiking inputs is not straightforward. However, for LTI systems, the effect of a Dirac impulse on the connected system, and thus the expression of the solution of system (1) with input u in (7), is well defined using the convolution integral and the well-known sifting property. Moreover, in view of the Dirac function definition, the spiking signal in (7) implies that the control input u is different from zero only at the spiking times and thus system (1) evolves in open loop between two spiking control instants, i.e., $\dot{x}(t) = Ax(t)$ for all $t \in [t_j, t_{j+1})$, $j \in \mathbb{Z}_{\geq 0}$, and the solution has a fixed-amplitude discontinuity at the spiking times $t_j \in \mathbb{R}_{\geq 0}$, i.e., $x(t_j^+) = x(t_j) + B\alpha_1$ or $x(t_j^+) = x(t_j) - B\alpha_2$ depending on which neuron generates the spike at time t_j .

Now that we have proposed the neuromorphic controller and provided a suitable modeling framework, it is our objective to derive conditions on the neuron parameters α_ℓ and Δ_ℓ , $\ell \in \{1, 2\}$, to guarantee a formal practical stability property of system (1) with spiking input (7), which is the closed-loop system considered in this paper. For this purpose we follow an emulation-based approach, as described in the next section.

Remark 1. *Equations (6) and (7) assume that the actuator (embedded in the linear time-invariant model) can cope with spiking control signals, which is reasonable in various applications, see, e.g., [3], [37]. Interestingly, the number and type of neuromorphic devices, such as actuators and sensors, which are important for the real-life implementation of neuromorphic controllers are growing in the recent years due the engineering community's interest in developing neuromorphic closed-loop systems. Moreover, modeling spikes as Dirac impulses is a modeling idealization, which is reasonable in view of the different time scale of spikes compared to the system dynamics, as also done in [12], [16], [21], [30].*

Remark 2. *We cannot apply the results on singular perturbation or averaging for hybrid systems, see, e.g., [38], [39] to ensure a stability property of the closed-loop system (1) with spiking input (7). Indeed, in the considered neuromorphic control setting the required time-scale separation is not present because the jumps (spikes) are generated by the fast dynamics (neurons) and the (possibly) slow dynamics (plant) are directly affected by the (fast) spikes. In this paper, we therefore develop a new method to prove the desired closed-loop properties, also leading to explicit and quantitative bounds. Note that singular perturbation theory typically provides only qualitative bounds.*

IV. EMULATION-BASED NEUROMORPHIC CONTROLLER

To ensure a stability property of the closed-loop system with a spiking controller we follow an emulation-based approach in the sense that we first assume that we know a stabilizing continuous-time controller for a LTI system (see Assumption 1) and then we design the spiking neural network (SNN) to approximate the closed-loop behavior we would have obtained if the system had been controlled using the stabilizing continuous-time controller.

For SISO LTI systems Assumption 1 implies that there exists $K \in \mathbb{R}$ such that $A + BKC$ is Hurwitz, with $A \in$

$\mathbb{R}^{n_x \times n_x}$, $B \in \mathbb{R}^{n_x \times 1}$ and $C \in \mathbb{R}^{1 \times n_x}$ from (1). Moreover, without loss of generality, we assume $K \in \mathbb{R}_{>0}$. When Assumption 1 is satisfied for some $K \in \mathbb{R}_{<0}$, then such a positive K exists because we can then flip the sign of the generated control input. The goal of our emulation-based design approach is to approximate the closed-loop trajectories of the “ideal” closed-loop system

$$\dot{\bar{x}} = (A + BKC)\bar{x} = \bar{A}\bar{x}, \quad (8)$$

with $\bar{A} := (A + BKC) \in \mathbb{R}^{n_x \times n_x}$ and $\bar{x}(0) = x_0 \in \mathbb{R}^{n_x}$. For this purpose, we consider the difference $\tilde{x} := x - \bar{x} \in \mathbb{R}^{n_x}$ between the closed-loop trajectory x given by (1) with the spiky controller generating (7) and the trajectory \bar{x} of the ideal continuous-time closed loop in (8). This difference \tilde{x} , which we also call the state emulation error, is governed by

$$\begin{aligned} \dot{\tilde{x}} &= \dot{x} - \dot{\bar{x}} \stackrel{(1),(8)}{=} Ax + Bu - (A + BKC)\bar{x} \\ &= Ax + BKCx - BKCx + Bu - (A + BKC)\bar{x} \quad (9) \\ &= (A + BKC)\tilde{x} - BKCx + Bu \\ &= \bar{A}\tilde{x} - Be, \end{aligned}$$

with $\tilde{x}(0) = x(0) - \bar{x}(0) = x_0 - x_0 = 0$, and $e := KCx - u \in \mathbb{R}$ the emulation error. Since $\tilde{x}(0) = 0$ and \bar{A} is Hurwitz from Assumption 1, from (9) we have that the trajectory of system (1) with spiking input (7) approximates the desired closed-loop trajectory \bar{x} , i.e., \tilde{x} is bounded, if the emulation error e is bounded and small. Note that $e(t) = Ky(t) \in \mathbb{R}$ for all $t \in [t_j, t_{j+1})$, $j \in \mathbb{Z}_{\geq 0}$, and at the spiking times t_j , $j \in \mathbb{Z}_{>0}$, e has Dirac impulses due to the spikes in u from (7). Moreover $Ky = KCx$ could be discontinuous at the spiking times t_j , $j \in \mathbb{Z}_{>0}$. Hence, e will not be small in a standard Euclidean sense and an alternative (integral) metric will be proposed and used for this purpose in Theorem 1 and Definition 1 below. Thus, our goal is to provide conditions on the neurons parameters α_ℓ , Δ_ℓ such that the spiking signal u from (7) emulates, in a sense that will be clarified below, the signal Ky with K as in Assumption 1. We also stress that the proposed neuromorphic controller does not need to implement Ky and only the knowledge of the stabilizing gain $K \in \mathbb{R}_{>0}$ is required for its design and implementation.

To guarantee a practical stability property of system (1) with $n_u = n_y = 1$ in closed loop with the two-neuron spiking controller generating (7), we use a two-step approach:

Step 1: We provide conditions on the neuron parameters α_ℓ and Δ_ℓ , $\ell \in \{1, 2\}$, to guarantee an upperbound on the norm of the integral of the emulation error e . This bound uses a new metric to formally study a *signal-based* version of a *universal approximation property* of two-neuron integrate-and-fire spiking neural networks (see Section V), which is useful to prove a closed-loop stability property for system (1) with spiking input (7) in Step 2.

Step 2: We show that an asymptotically stable LTI system with spiking input, such as (9) with $\bar{A} \in \mathbb{R}^{n_x \times n_x}$ Hurwitz, satisfies a new type of integral input-to-state stability, for which we introduce the term *integral Spiking Input-to-State Stability* (iSISS) (see Section VI), relating to the metric used in the first step.

By combining Steps 1 and 2, we can guarantee an arbitrary small bound on the state emulation error \tilde{x} in (9). This result can be used to obtain a practical stability property of system (1) with spiking input (7) (see Section VII).

V. APPROXIMATION PROPERTIES OF INTEGRATE-AND-FIRE SPIKY NEURAL NETWORKS

The goal of this section is to prove a signal-based version of a universal approximation property for the two-neuron spiking network in (2)-(7).

For this purpose, we first establish well-posed behavior of the neuron in the sense that in the next proposition, whose proof is given in Appendix A, we ensure that the spiking signal u_ℓ in (7) generated by the neuron $\ell \in \{1, 2\}$ is such that no accumulation of spiking times can happen. Since the number of neurons is finite, this property implies that there is no accumulation of the spiking times in the overall spiking sequence $\{t_j\}_{j \in \mathbb{Z}_{\geq 0}} = \{t_{1,j_1}\}_{j_1 \in \mathbb{Z}_{\geq 0}} \cup \{t_{2,j_2}\}_{j_2 \in \mathbb{Z}_{\geq 0}}$. This property excludes the Zeno phenomenon and ensures that solutions to system (1) with spiking input u in (7) are well-defined. This is an important property which will be essential in Sections VI and VII to guarantee stability of the closed-loop system (1), (7). Moreover, this property can be proven following similar lines for any network with finite number of integrate-and-fire neurons.

Proposition 1. *Consider neuron $\ell \in \{1, 2\}$ in (2)-(5), where $y \in \mathcal{L}_{\mathbb{R}}$ is its signal input. Then, the sequence of spiking times $\{t_{\ell,j_\ell}\}_{j_\ell \in \mathbb{Z}_{\geq 0}}$ in (4), is such that $j_\ell < \infty$ or it satisfies, $t_{\ell,j_\ell} \rightarrow +\infty$ as $j_\ell \rightarrow +\infty$ for all $\ell \in \{1, 2\}$ and all $\xi_\ell(0) \in [0, \Delta_\ell]$. Moreover, the sequence of spiking times $\{t_j\}_{j \in \mathbb{Z}_{\geq 0}} = \{t_{1,j_1}\}_{j_1 \in \mathbb{Z}_{\geq 0}} \cup \{t_{2,j_2}\}_{j_2 \in \mathbb{Z}_{\geq 0}}$ is such that $j < \infty$ or it satisfies $t_j \rightarrow \infty$ as $j \rightarrow \infty$ for all $\xi_\ell(0) \in [0, \Delta_\ell]$, $\ell \in \{1, 2\}$.*

In the next theorem we ensure a signal-based version of the universal approximation property.

Theorem 1. *Consider the two-neuron integrate-and-fire spiking neural network in (2)-(7), where $y \in \mathcal{L}_{\mathbb{R}}$ is a signal input to the neurons. Then, for any $t \in \mathbb{R}_{\geq 0}$, and each $\ell \in \{1, 2\}$,*

$$\left| \int_0^t \max \{0, (3 - 2\ell)K_\ell y(s)\} - (3 - 2\ell)u_\ell(s)ds \right| \leq \alpha_\ell, \quad (10)$$

with u_ℓ defined in (6), and $K_\ell = \frac{\alpha_\ell}{\Delta_\ell}$. Moreover, for any $t \in \mathbb{R}_{\geq 0}$,

$$\left| \int_0^t \psi(s)ds \right| \leq \alpha_1 + \alpha_2, \quad (11)$$

with $\psi(t) = \max \{0, K_1 y(t)\} - \max \{0, -K_2 y(t)\} - u(t) \in \mathbb{R}$, $t \in \mathbb{R}_{\geq 0}$, where u is defined in (7). Moreover, in case $\xi_\ell(0) = 0$, $\ell \in \{1, 2\}$, then

$$\left| \int_0^t \psi(s)ds \right| \leq \max \{\alpha_1, \alpha_2\}, \quad (12)$$

for any $t \in \mathbb{R}_{\geq 0}$.

Theorem 1, whose proof is given in Appendix B, formally establishes important approximation properties for an integrate-and-fire neuron outputting spiky signals in a “super-integral” sense. Note that, the bound is given by α_ℓ , and thus

can be made arbitrary small for fixed K_ℓ if there is freedom in the selection of the neuron’s firing threshold Δ_ℓ and spike amplitude α_ℓ . Moreover, Theorem 1 also ensures a bound, given by $\alpha_1 + \alpha_2$, (or $\max\{\alpha_1, \alpha_2\}$) on the norm of the integral of $\psi(t) = \max \{0, K_1 y(t)\} - \max \{0, -K_2 y(t)\} - u(t)$, for any $t \in \mathbb{R}_{\geq 0}$, with $u(t)$ defined in (7) and thus it formally guarantees an approximation property for the two-neuron network in (2)-(7). Note that, (10) shows that the spiking signal output of neuron $\ell \in \{1, 2\}$, approximates the function $\max \{0, (3 - 2\ell)K_\ell y(s)\}$, which is known as Rectifier Linear Unit (ReLU), see, e.g., [40], [41], and is a well-known activation function in artificial neural networks (ANNs). Hence, Theorem 1 provides a formal link between feedforward ANNs and spiking neural networks (SNNs), where each integrate-and-fire neuron emulates a node of an ANN with a ReLU activation function.

The results of Theorem 1 can be used to emulate the static output feedback controller from Assumption 1. Indeed, a special case of Theorem 1 is when $K_1 = \frac{\alpha_1}{\Delta_1} = K_2 = \frac{\alpha_2}{\Delta_2} = K \in \mathbb{R}_{>0}$. In this case, for any $y \in \mathbb{R}$ we have $Ky = \max \{0, Ky\} - \max \{0, -Ky\}$ and thus we have, for all $t \in \mathbb{R}_{\geq 0}$,

$$\left| \int_0^t \tilde{\psi}(s)ds \right| \leq \alpha_1 + \alpha_2, \quad (13)$$

with $\tilde{\psi}(t) = Ky(t) - u(t)$, $t \in \mathbb{R}_{\geq 0}$. This special case of Theorem 1 extends the result in the preliminary conference version of this work [30, Theorem 1], allowing $\xi_\ell(0) \in [0, \Delta_\ell]$, not only $\xi_\ell(0) = 0$, $\ell \in \{1, 2\}$. Moreover, this special case (with $K_1 = K_2 = K$) of Theorem 1 will be used in Section VII to ensure that \tilde{x} in (9) is tunable and small, i.e., the difference \tilde{x} between the state x of the spiky control loop and the state \bar{x} of the “ideal” continuous-time system (8) remains small. As (8) is asymptotically stable, this will imply a global practical stability property of system (1) with input (7).

VI. INTEGRAL SPIKING INPUT-TO-STATE STABILITY PROPERTY FOR LTI SYSTEMS

In this section we introduce the *integral Spiking Input-to-State Stability* (iSIS) property, which will be instrumental to ensure a stability property for systems controlled by spiking controllers, and we compare it with the notion of integral input-to-state stability property presented in [28], [29]. We then show that an asymptotically stable LTI system, like the one we consider in (9), satisfies this stability property with respect to a class of spiking inputs, like e in (9), which is defined below.

Definition 1. *A signal v defined on $\mathbb{R}_{\geq 0}$ is a spiking signal, denoted by $v \in \mathcal{S}^{n_v}$, if it can be written as*

$$v = v_1 + v_2, \quad (14)$$

where $v_1 \in \mathcal{L}_{\mathbb{R}^{n_v}}$, and $v_2(t) := \sum_{i=1}^{\infty} \Theta_i \delta(t - t_i)$ with $t \in \mathbb{R}_{\geq 0}$ is a sequence of Dirac pulses with $\Theta_i \in \mathbb{R}^{n_v}$ for all $i \in \mathbb{Z}_{>0}$, and $\{t_i\}_{i \in \mathbb{Z}_{>0}}$ is a sequence of spiking times such that $t_{i+1} > t_i$, with $t_0 = 0$, for all $i \in \mathbb{Z}_{\geq 0}$ and $t_i \rightarrow \infty$ when $i \rightarrow \infty$, and v satisfies

$$\|v\|_* := \sup_{t \in \mathbb{R}_{\geq 0}} \left| \int_0^t v(s)ds \right| < +\infty, \quad (15)$$

where $\int_0^t v(s)ds = \int_0^t v_1(s)ds + \int_0^t v_2(s)ds$, where $\int_0^t v_1(s)ds$ denotes the Lebesgue integral from 0 to $t \in \mathbb{R}_{\geq 0}$ of $v_1 \in \mathcal{L}_{\mathbb{R}^{n_v}}$ and $\int_0^t v_2(s)ds = \sum_{i \in \mathbb{Z}_{>0}, t_i \in [0, t]} \Theta_i$.

The proof that $\|v\|_*$ in (15) is a norm on \mathcal{S}^{n_v} is given in Appendix E. Note that, the emulation error signal e , defined in Section IV, belongs to the class of spiking signals \mathcal{S}^1 defined in Definition 1 (with $n_v = 1$). Indeed, $e = Ky - u$, with u the spiking input in (7) and Ky , with $K \in \mathbb{R}$ from Assumption 1 with $n_u = n_y = 1$, is a Lebesgue measurable and locally essentially bounded function, as required by Definition 1. Moreover, from Theorem 1, we have $\|e\|_* \leq \alpha_1 + \alpha_2 < +\infty$. In addition, from Proposition 1 it follows that $t_i \rightarrow +\infty$ when $i \rightarrow +\infty$, as required by Definition 1.

Since we have a bound on the emulation error in the norm $\|\cdot\|_*$ and a particular signal class \mathcal{S} , we need a new definition of (integral) input-to-state stability [28]. This is proposed next. Although we focus on LTI systems in this paper, the iSISS property can be defined for general nonlinear systems of the form

$$\dot{z} = f(z, v), \quad (16)$$

with $z \in \mathbb{R}^{n_z}$ and $v \in \mathcal{S}^{n_v}$, $n_z, n_v \in \mathbb{Z}_{>0}$, provided that solutions to (16) with $z(0) = z_0 \in \mathbb{R}^{n_z}$ and spiking input $v \in \mathcal{S}^{n_v}$ are well-defined, exist on $\mathbb{R}_{\geq 0}$ and are unique.

Definition 2. System (16) is integral spiking-input-to-state stable (iSISS), if there exist functions $\gamma \in \mathcal{K}$ and $\beta \in \mathcal{KL}$ such that, for any $z(0) = z_0 \in \mathbb{R}^{n_z}$ and all $v \in \mathcal{S}^{n_v}$, the corresponding solution z is defined for all $t \in \mathbb{R}_{\geq 0}$ and satisfies

$$|z(t)| \leq \beta(|z_0|, t) + \gamma(\|v\|_*) \quad (17)$$

for all $t \in \mathbb{R}_{\geq 0}$.

Definition 2 provides the iSISS property for system (16) with respect to spiking inputs only when the solutions are well-defined. For LTI systems as in (1) with input (7), solutions are well-defined as indicated in Section III before. This is not straightforward for a general nonlinear system in the form (16), see, e.g., [42]. However, the notion of solution is properly defined for some classes of nonlinear systems, e.g., $\dot{z} = f(z) + Gv$. Definition 2 implies that when system (16) is iSISS, then the norm of solution obtained starting from the initial condition $z_0 \in \mathbb{R}^{n_z}$, with input signal $v \in \mathcal{S}^{n_v}$ converges to a neighborhood of the origin, whose size is determined by $\gamma(\|v\|_*)$, as $t \rightarrow +\infty$.

Remark 3. The “classical” notion of integral input-to-state stability (iISS) for system (16) with input v in [28], [29] differs from Definition 2 because it considers $\int_0^\infty \gamma(|v(s)|)ds$ instead of $\gamma(\|v\|_*)$, with $\|v\|_* = \sup_{t \in \mathbb{R}_{\geq 0}} |\int_0^t v(s)ds|$ in (17). Note the different position of the norm and $\gamma \in \mathcal{K}$. Moreover, the iSISS admits a larger class of input signals, including “Dirac spikes”. Indeed, for instance, the emulation error defined in Section IV is such that $\|e\|_*$ is finite, but $\|e\|_1 = \int_0^\infty |e(s)|ds \in \mathbb{R}_{\geq 0}$ is typically not. When the iSISS property in Definition 2 holds with linear gain, i.e., $\gamma \in \mathcal{K}$ such that $\gamma(s) = \tilde{\gamma}s$, for some $\tilde{\gamma} \in \mathbb{R}_{\geq 0}$ for all $s \in \mathbb{R}_{\geq 0}$ then, $\int_0^\infty \gamma|v(s)|ds = \gamma \int_0^\infty |v(s)|ds$. In this

case, the iSISS property implies the “classical” iISS property. Indeed, the inequality in (17) is stronger than the inequality $|z(t)| \leq \beta(|z_0|, t) + \gamma\|v\|_1$, for signals for which $\|v\|_1 = \int_0^\infty |v(s)|ds \in \mathbb{R}_{\geq 0}$ is finite (and thus $\|v\|_*$ is finite) as $\|v\|_* = \sup_{t \in \mathbb{R}_{\geq 0}} |\int_0^t v(s)ds| \leq \sup_{t \in \mathbb{R}_{\geq 0}} \int_0^t |v(s)|ds = \|v\|_1$. Thus, in the linear iSISS gain case, the iSISS property is a stronger property than the iISS.

We will now prove that iSISS holds for an asymptotically stable LTI system.

Theorem 2. Consider system (16) with $f(z, v) = Fz + Gv$, and $F \in \mathbb{R}^{n_z \times n_z}$ Hurwitz and $G \in \mathbb{R}^{n_z \times n_v}$. Then it is iSISS with $\beta \in \mathcal{KL}$ given by $\beta(r, s) := ce^{-\lambda s}r$, $r, s \in \mathbb{R}_{\geq 0}$, for some $c, \lambda \in \mathbb{R}_{>0}$, and $\gamma \in \mathcal{K}$ given by $\gamma(s) = \tilde{\gamma}s \in \mathcal{K}$, $s \in \mathbb{R}_{\geq 0}$, with $\tilde{\gamma} := \|G\| + \int_0^\infty \|Fe^{Fs}G\| ds \in \mathbb{R}_{\geq 0}$.

VII. PRACTICAL STABILITY PROPERTY OF THE CLOSED-LOOP SYSTEM

By exploiting the results from Theorems 1 and 2, we first show in Theorem 3 below that the trajectory of system (1) with spiking input (7) remains (tunably) close to the ideal continuous-time closed-loop trajectory (8) from the same initial state. From this new contribution, we can ensure a practical stability property for LTI systems in closed loop with spiking controllers (see Corollary 1 below).

Theorem 3. Consider system (1) with $n_u = n_y = 1$ and suppose that Assumption 1 holds with $K \in \mathbb{R}_{>0}$. Let u be given by (7) using (2)-(6) with $\alpha_\ell \in \mathbb{R}_{>0}$ and $\Delta_\ell \in \mathbb{R}_{>0}$, $\ell \in \{1, 2\}$, in (4), (6) such that $K = \frac{\alpha_\ell}{\Delta_\ell}$, $\ell \in \{1, 2\}$. Define $\tilde{x} = x - \bar{x}$ as in (9), with \bar{x} from (8). Then, for any $x(0) = \bar{x}(0) \in \mathbb{R}^{n_x}$, and any $\xi_\ell(0) \in [0, \Delta_\ell]$, $\ell \in \{1, 2\}$, it holds that

$$|\tilde{x}(t)| \leq \gamma(\alpha_1 + \alpha_2), \quad (18)$$

for all $t \in \mathbb{R}_{\geq 0}$, where $\gamma := \|B\| + \int_0^\infty \|\bar{A}e^{\bar{A}s}B\| ds \in \mathbb{R}_{\geq 0}$. Moreover, if $\xi_1(0) = \xi_2(0) = 0$, then for any $x(0) = \bar{x}(0) = x_0 \in \mathbb{R}^{n_x}$, for all $t \in \mathbb{R}_{\geq 0}$,

$$|\tilde{x}(t)| \leq \gamma \max\{\alpha_1, \alpha_2\}. \quad (19)$$

All technical proofs are in the Appendix, except the proof of this theorem and the next corollary as they provide insights in our conceptual approach relying on Theorem 1 and Theorem 2.

Proof. Let all conditions of Theorem 3 hold. Using $\tilde{x} = x - \bar{x}$, from (9) we have

$$\dot{\tilde{x}} = \bar{A}\tilde{x} - Be, \quad (20)$$

where $\bar{A} = (A + BKC) \in \mathbb{R}^{n_x \times n_x}$ is Hurwitz with $K = \frac{\alpha_\ell}{\Delta_\ell}$, $\ell \in \{1, 2\}$, from Assumption 1, and $e = Ky - u$, where $Ky = \max\{0, Ky\} - \max\{0, -Ky\}$ and u in (7).

Since $x(0) = \bar{x}(0)$, it holds that $\tilde{x}(0) = 0$. From Theorem 2 we obtain, for all $t \in \mathbb{R}_{\geq 0}$,

$$|\tilde{x}(t)| \leq \left(\|B\| + \int_0^\infty \|\bar{A}e^{\bar{A}s}B\| ds \right) \|e\|_* = \gamma \|e\|_*. \quad (21)$$

Moreover, from Theorem 1 we have that for all $t \in \mathbb{R}_{\geq 0}$, $\left| \int_0^t e(s)ds \right| \leq \alpha_1 + \alpha_2$. Therefore

$$\|e\|_* = \sup_{t \in \mathbb{R}_{\geq 0}} \left| \int_0^t e(s)ds \right| \leq \alpha_1 + \alpha_2, \quad (22)$$

which, from (21) implies $|\tilde{x}(t)| \leq \gamma(\alpha_1 + \alpha_2)$.

Similarly, in case $\xi_1(0) = \xi_2(0) = 0$, from Theorem 1, (22) can be replaced by $\|e\|_* \leq \max\{\alpha_1, \alpha_2\}$, which, combined with (21), implies (19). This concludes the proof. \square

Theorem 3 shows that the trajectories x of the spiky closed-loop system and the corresponding trajectories \bar{x} to the “ideal” loop $\dot{\bar{x}} = \bar{A}\bar{x}$ for the same initial condition remain close according to the bounds in (18) or (19) for all times. Recall that, as discussed after Theorem 1, we can tune the bound on the state emulation error \tilde{x} by making $\alpha_\ell, \ell \in \{1, 2\}$, small. As a consequence, using the definition of $\tilde{x} = x - \bar{x}$, in the next corollary we can ensure a practical stability property of system (1) with spiking input (7).

Corollary 1. *Consider system (1) with $n_u = n_y = 1$ and suppose that Assumption 1 holds with $K \in \mathbb{R}_{>0}$. Let u be given by (7) using (2)-(6) with $\alpha_\ell \in \mathbb{R}_{>0}$ and $\Delta_\ell \in \mathbb{R}_{>0}$, $\ell \in \{1, 2\}$, in (4), (6) such that $K = \frac{\alpha_\ell}{\Delta_\ell}$, $\ell \in \{1, 2\}$. Then, for any $x(0) = x_0 \in \mathbb{R}^{n_x}$, and any $\xi_\ell(0) \in [0, \Delta_\ell]$, $\ell \in \{1, 2\}$, for all $t \in \mathbb{R}_{\geq 0}$,*

$$|x(t)| \leq \beta(|x_0|, t) + \gamma(\alpha_1 + \alpha_2), \quad (23)$$

with $\beta(r, s) = ce^{-\lambda s}r$, $r, s \in \mathbb{R}_{\geq 0}$, for some $c, \lambda \in \mathbb{R}_{>0}$, and $\gamma := \|B\| + \int_0^\infty \|\bar{A}e^{\bar{A}s}B\| ds \in \mathbb{R}_{\geq 0}$. Moreover, if $\xi_1(0) = \xi_2(0) = 0$, then for any $x(0) = x_0 \in \mathbb{R}^{n_x}$, for all $t \in \mathbb{R}_{\geq 0}$,

$$|x(t)| \leq \beta(|x_0|, t) + \gamma \max\{\alpha_1, \alpha_2\}. \quad (24)$$

Proof. The proof follows directly from Theorem 3 providing a bound on $\tilde{x} = x - \bar{x}$ and the asymptotic stability of $\dot{\bar{x}} = \bar{A}\bar{x}$. Indeed, for all $t \in \mathbb{R}_{\geq 0}$, we get

$$|x(t)| = |\bar{x}(t) + \tilde{x}(t)| \leq |\bar{x}(t)| + |\tilde{x}(t)|. \quad (25)$$

In view of Assumption 1, $\bar{A} = A + BKC$ is Hurwitz and thus, there exist $c, \lambda \in \mathbb{R}_{>0}$ such that $|\bar{x}(t)| \leq ce^{-\lambda t}|\bar{x}(0)| = \beta(|\bar{x}(0)|, t)$, for all $t \in \mathbb{R}_{\geq 0}$. Using $\bar{x}(0) = x(0) = x_0 \in \mathbb{R}^{n_x}$, and the bound on $|\tilde{x}|$ from (18) and (19), from (25), we obtain (23) and (24), respectively. \square

Corollary 1 guarantees that the state of the closed-loop system (1), (7), with (7) generated by a two-neuron SNN designed to emulate a stabilizing static-output feedback controller (see Assumption 1), converges to a neighborhood of the origin, a ball of radius $\gamma(\alpha_1 + \alpha_2)$ (or $\gamma \max\{\alpha_1, \alpha_2\}$ if $\xi_\ell(0) = 0$, $\ell \in \{1, 2\}$), as time grows. Interestingly, note that the β in the corollary is related only to the dynamics of $\dot{\bar{x}} = \bar{A}\bar{x}$ and, hence, it inherits its properties, e.g., convergence rates, in a practical sense.

It is worth noticing again that, since the only condition required in Corollary 1 is $K = \alpha_\ell/\Delta_\ell$, $\ell \in \{1, 2\}$, it is possible to select α_ℓ and Δ_ℓ such that the ultimate bound

$\gamma(\alpha_1 + \alpha_2)$ (or $\gamma \max\{\alpha_1, \alpha_2\}$) is arbitrarily small by choosing α_ℓ , $\ell \in \{1, 2\}$, arbitrarily small, at the cost of also picking the firing threshold Δ_ℓ arbitrarily small, which implies that the spikes are typically generated more frequently, see also the proof of Proposition 1. In view of the structure of the spiking controller, which leaves the system plant in open loop between spikes, if the matrix A in (1) is unstable, an asymptotic stability property cannot be obtained and thus a practical stability property is the best we can ensure.

Theorem 3 (and Corollary 1) and its proof rely conceptually on the signal-based universal approximation property guaranteed by Theorem 1 and on the iSISS property proven in Theorem 2. Following similar steps, it is possible to prove a practical stability property for any iSISS system in closed loop with a spiking controller satisfying the bound on the emulation error in Theorem 1. Thus, the two-step approach we have presented in this paper has potential to be generalized for larger classes of systems and/or different type of neurons, as long as the properties in Theorems 1 and 2 are ensured.

In the next section, we discuss the generalization to MIMO LTI systems.

Remark 4. *From an implementation perspective, small perturbations in the neurons’ parameters α_ℓ and Δ_ℓ , $\ell \in \{1, 2\}$, do not compromise the practical stability property ensured by Corollary 1. Indeed, such perturbations imply that the spiking input generated by the neuromorphic controller emulates a static output feedback control input $\tilde{K}y$, where \tilde{K} remains close to the original gain K from Assumption 1. Hence, as long as $A + B\tilde{K}C$ is Hurwitz, a practical stability property is preserved. As eigenvalues of $A + B\tilde{K}C$ depends continuously on \tilde{K} , this shows an intrinsic robustness property of the proposed approach for stabilizing LTI systems.*

VIII. GENERALIZATIONS

In this section we discuss generalizations and extensions of the presented results. In Section VIII-A we consider multi-input multi-output (MIMO) LTI systems, emulating static output (or state) feedback control, and we discuss how the network has to be modified in this case to ensure a practical stability property. In Section VIII-B we generalize the approximation property illustrated in Section V to approximate any continuous piecewise affine function using an integrate-and-fire spiking neuronal network (SNN) with more than two neurons. This property will allow us to emulate a larger class of static controllers, which could be useful to globally stabilize nonlinear systems. Note that the approximation property of integrate-and-fire SNNs in Sections V and VIII-B are independent on the system we aim to stabilize. Thus, if solutions to a nonlinear plant with spiking input signal are well defined, we just need an iSISS property, as in Definition 2, and then we can apply the proposed technique to approximate a globally stabilizing continuous-time control input with a spiking signal.

A. MIMO LTI systems

In Sections III-VII we focused on SISO LTI systems. We now generalize the results for MIMO LTI systems, e.g., (1)

with $u := (u_1, u_2, \dots, u_{n_u}) \in \mathbb{R}^{n_u}$, $y := (y_1, y_2, \dots, y_{n_y}) \in \mathbb{R}^{n_y}$, with $n_u, n_y \in \mathbb{Z}_{>0}$, for which a MIMO version of Assumption 1 is satisfied. In this case, to prove a practical stability property, the control input to emulate is given by $\hat{u} := Ky$, with

$$K = \begin{bmatrix} K_{1,1} & K_{1,2} & \dots & K_{1,n_y} \\ K_{2,1} & K_{2,2} & \dots & K_{2,n_y} \\ \vdots & \vdots & & \vdots \\ K_{n_u,1} & K_{n_u,2} & \dots & K_{n_u,n_y} \end{bmatrix} \in \mathbb{R}^{n_u \times n_y}. \quad (26)$$

Each component of the control input $\hat{u} = (\hat{u}_1, \hat{u}_2, \dots, \hat{u}_{n_u}) \in \mathbb{R}^{n_u}$ we want to emulate is given by

$$\hat{u}_i = \sum_{j=1}^{n_y} K_{i,j} y_j, \quad i \in \{1, 2, \dots, n_u\}. \quad (27)$$

We can therefore design a network composed of $2n_u n_y$ integrate-and-fire neurons, with dynamics, similarly to (2),

$$\dot{\xi}_{\ell,i,j} = \max\{0, (3 - 2\ell)y_j\}, \quad (28)$$

with $\xi_{\ell,i,j}(0) \in [0, \Delta_{\ell,i,j}]$, $\Delta_{\ell,i,j} \in \mathbb{R}_{>0}$, $\ell \in \{1, 2\}$, $i \in \{1, 2, \dots, n_u\}$ and $j \in \{1, 2, \dots, n_y\}$. Neuron $\xi_{\ell,i,j}$ generates spikes with amplitude $\alpha_{\ell,i,j} \in \mathbb{R}_{>0}$ whenever $\xi_{\ell,i,j} \geq \Delta_{\ell,i,j}$, similarly to (5). For each $i \in \{1, 2, \dots, n_u\}$, the spiking output of the $2n_y$ neurons (with the same i) is summed up to obtain a spiking input u_i . Note that, since the neuron dynamics in (28) is the same as in (2) and the input to the neuron is $y_j \in \mathcal{L}_{\mathbb{R}}$, $j \in \{1, 2, \dots, n_y\}$, a result similar to the one in Proposition 1 can be proven for each neuron of the network. Thus, since the number of neurons is finite (equal to $2n_u n_y$), the signal u_i , $i \in \{1, 2, \dots, n_u\}$, is such that no accumulation of spiking times can happen, and is a spiking signal, according to Definition 1. By selecting the neurons parameters such that $K_{i,j} = \frac{\alpha_{\ell,i,j}}{\Delta_{\ell,i,j}}$ and using Theorem 1 for each pair of neurons (with same i and j), we can prove that u_i emulates \hat{u}_i in (27) in the sense that, for each $i \in \{1, 2, \dots, n_u\}$, for all $t \in \mathbb{R}_{\geq 0}$,

$$\left| \int_0^t \hat{u}_i(s) - u_i(s) ds \right| \leq \sum_{j=1}^{n_y} (\alpha_{1,i,j} + \alpha_{2,i,j}). \quad (29)$$

Recalling the definition of the emulation error $e = \hat{u} - u \in \mathcal{S}^{n_u}$ and using (30) for each $i \in \{1, 2, \dots, n_u\}$, we obtain

$$\|e\|_* \leq \sqrt{\sum_{i=1}^{n_u} \left(\sum_{j=1}^{n_y} (\alpha_{1,i,j} + \alpha_{2,i,j}) \right)^2}. \quad (30)$$

Note that, similarly to Theorem 1, the bound on the emulation error depends on the spikes' amplitudes $\alpha_{\ell,i,j} \in \mathbb{R}_{>0}$, and thus can be made arbitrarily small if there is freedom in selecting the thresholds $\Delta_{\ell,i,j}$.

The bound on the emulation error (30) can be combined with the iSISS property in Section VI and, following similar steps as in Section VII, a small state emulation error \tilde{x} between x and the solution to $\dot{\tilde{x}} = (A + BKC)\tilde{x}$ can be guaranteed (similarly to Theorem 3) next to a practical stability property of the closed-loop system (as in Corollary 1 using (30)).

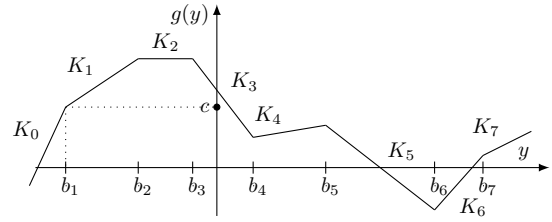


Fig. 2. Example of piecewise linear function g in (32) with $N = 7$.

Remark 5. The MIMO implementation consists of a one-layer integrate-and-fire SNN with $2n_u n_y$ neurons, where only unit gains are used in the signals. The network structure is as the one in Fig. 1 repeated $n_u n_y$ times. In particular, each neuron has only the positive or negative part of a signal y_j as input. In case we allow non-unit gains and, hence, weighted combinations of the measured outputs y_1, y_2, \dots, y_{n_y} to flow into the neuron dynamics, we can use our emulation-based approach to directly emulate the signals $\hat{u}_i = K_{i,\bullet} y$ in (27) by a pair of neurons with spike amplitudes $\alpha_{1,i}$ and $\alpha_{2,i}$. Here $K_{i,\bullet}$ denotes the i -th row of K , $i = 1, \dots, n_u$. Note that in this case we take the spike amplitudes $\alpha_{1,i}$, $\alpha_{2,i}$ and firing thresholds $\Delta_{1,i}$, $\Delta_{2,i}$ such that $\frac{\alpha_{\ell,i}}{\Delta_{\ell,i}} = 1$, $\ell \in \{1, 2\}$, $i \in \{1, 2, \dots, n_u\}$ (such that the neurons have “unit gain”). This leads to a one-layer integrate-and-fire SNN with $2n_u$ neurons that have as inputs the positive or negative parts of $K_{i,\bullet} y$ (so weighted versions of the inputs). This would reduce not only the number of neurons, but also changes the bound (29) to

$$\left| \int_0^t \hat{u}_i(s) - u_i(s) ds \right| \leq \alpha_{1,i} + \alpha_{2,i}, \quad (31)$$

which is significantly smaller. The lower number of neurons would overall also generate less spikes. This underlines that the emulation results in this paper can be used for various neural network structures (with or without unit gains). Depending on the network structure and also the controller gain K that is emulated, the number of spikes can be smaller or larger. Optimal designs of the network structure and the choice of the to-be-emulated gain K (and values of firing thresholds and spike amplitudes) trading off convergence rates, ultimate error bounds and number of spikes is an interesting topic, left for future work.

Remark 6. The generalization presented in this section to emulate static output feedback controllers to stabilize MIMO LTI plants can be applied mutatis mutandi to emulate a static state feedback control input given by $\hat{u} = Kx$, with $K \in \mathbb{R}^{n_u \times n_x}$, using the neuromorphic controller. Indeed, in this case, we can simply write (26)-(30) for $y = x \in \mathbb{R}^{n_x}$. Moreover, when the full state is measured, i.e., $y = x$, if the pair (A, B) in (1) is stabilizable, then there exists $K \in \mathbb{R}^{n_u \times n_x}$ such that $(A + BK)$ is Hurwitz, namely $\hat{u} = Kx$ is a static state feedback control.

B. Approximation property for larger networks and arbitrary continuous piecewise affine functions

In Theorem 1, given any signal $y \in \mathcal{L}_{\mathbb{R}}$ input to an integrate-and-fire neuron $\ell \in \{1, 2\}$, we provided a condition on the

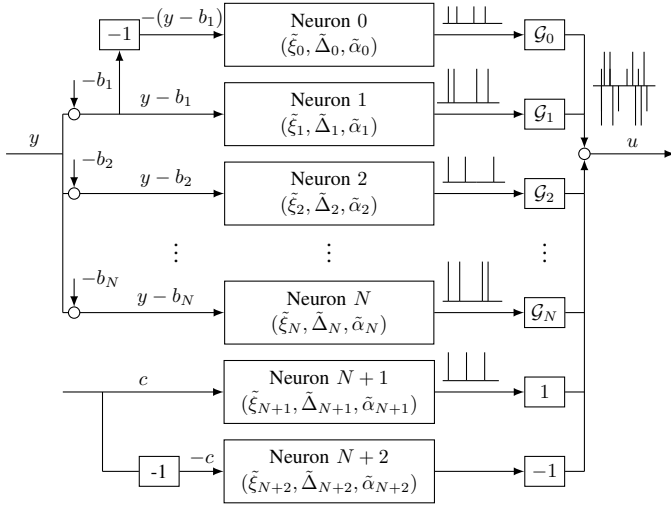


Fig. 3. Block diagram representing one-layer $(N+3)$ -neuron network, with input $y \in \mathbb{R}$ and spiking output $u \in \mathcal{S}$. $b_i \in \mathbb{R}$ are the bias of the network and $G_i \in \{-1, 1\}$ are gains that define the sign of the spiking output of each neuron. Note that, depending on the sign of the constant c only one among neurons ξ_{N+1} or ξ_{N+2} generates spikes.

neuron parameters α_ℓ and Δ_ℓ of the neuron $\ell \in \{1, 2\}$, in (2)-(7) so that the spiking output of the neuron ℓ approximates the function $\max\{0, (3-2\ell)K_\ell y\}$ in the sense of (10). As such, we formally showed how each node of an ANN with RELU activation functions is approximated using an integrate-and-fire neuron with arbitrary precision, assuming that the neuron parameters α_ℓ and Δ_ℓ can be chosen freely. In this section we generalize that result, by ensuring that a $(N+3)$ -neuron network, with $N \in \mathbb{Z}_{>0}$, approximates a *continuous* piecewise affine (PWA) function g , with $N+1$ affine pieces with slopes K_0 in range (b_0, b_1) , K_i , $i \in \{1, 2, \dots, N\}$ in range $[b_i, b_{i+1})$, where $b_i \in \mathbb{R}$, $i \in \{0, 1, \dots, N+1\}$, are such that $b_0 < b_1 \leq b_2 \leq \dots \leq b_N < b_{N+1}$, with $b_0 = -\infty$ and $b_{N+1} = +\infty$. Moreover $g(0) = c$, with $c \in \mathbb{R}$. An example of PWA function with $N = 7$ is given in Fig. 2. This function can be written as, for one-dimensional $y \in \mathcal{L}_{\mathbb{R}}$,

$$\begin{aligned} g(y) &= c - K_0 \max\{0, -(y - b_1)\} + K_1 \max\{0, y - b_1\} \\ &\quad + (K_2 - K_1) \max\{0, y - b_2\} + \dots \\ &\quad + (K_N - K_{N-1}) \max\{0, y - b_N\} \\ &= c - K_0 \max\{0, -(y - b_1)\} + K_1 \max\{0, y - b_1\} \\ &\quad + \sum_{i=2}^N (K_i - K_{i-1}) \max\{0, y - b_i\}. \end{aligned} \quad (32)$$

Note that any continuous PWA function can be written in the form (32) and is uniquely parametrized by N , c , b_i , $i \in \{1, 2, \dots, N\}$, and K_i , $i \in \{0, 1, \dots, N\}$.

To emulate the continuous PWA function in (32), we consider the neuronal network in Fig. 3, which is composed of $N+3$ neurons, denoted ξ_i , $i \in \{0, 1, \dots, N+2\}$, whose

dynamics is given by, similarly to (2)-(7),

$$\begin{aligned} \dot{\xi}_0 &= \max\{0, -(y - b_1)\} \\ \dot{\xi}_i &= \max\{0, y - b_i\}, \quad i \in \{1, 2, \dots, N\} \\ \dot{\xi}_{N+1} &= \max\{0, c\} \\ \dot{\xi}_{N+2} &= \max\{0, -c\}, \end{aligned} \quad (33)$$

where $c \in \mathbb{R}$ and $b_i \in \mathbb{R}$, $i \in \{1, 2, \dots, N\}$ comes from (32) and $\xi_i(0) \in [0, \tilde{\Delta}_i]$, $i \in \{0, 1, \dots, N+2\}$, with $\tilde{\Delta}_i \in \mathbb{R}_{>0}$ the firing threshold of neuron ξ_i . It is worth noticing that if $c = 0$, the last two neurons will never generate spikes. On the other hand, when $c \neq 0$, since it is a constant, only one among $\max\{0, c\}$ and $\max\{0, -c\}$ will be different from 0, and thus, one of these two neurons will never generate spikes. Therefore, if the sign of c is known (or if c is zero), the network could have $N+2$ (or $N+1$) neurons, instead of $N+3$, and one (or both) of these two neurons could be removed. Neuron ξ_i , $i \in \{0, 1, \dots, N+2\}$, generates a spike with amplitude $\tilde{\alpha}_i \in \mathbb{R}_{>0}$ whenever ξ_i reaches the threshold $\tilde{\Delta}_i \in \mathbb{R}_{>0}$. When this occurs, ξ_i is reset to 0. Gains $G_i \in \{-1, 1\}$, $i \in \{0, 1, \dots, N\}$, define the sign of the spiking signal u_i . Moreover $G_{N+1} = 1$ and $G_{N+2} = -1$. Similarly to (4) we denote the sequence of the spiking times generated by each neuron as $\{t_{i,j_i}\}_{j_i \in \mathbb{Z}_{>0}}$, $i \in \{0, 1, \dots, N+2\}$, which is defined as,

$$t_{i,0} = t_0 = 0, \quad t_{i,j_i+1} := \inf\{t > t_{i,j_i} : \xi_i(t) \geq \tilde{\Delta}_i\}. \quad (34)$$

Similar to (6), we define the spiking signal generated by each neuron as, for each $i \in \{0, 1, \dots, N+2\}$, and all $t \in \mathbb{R}_{\geq 0}$,

$$u_i(t) = \sum_{k=1}^{\infty} G_i \alpha_i \delta(t - t_{i,k}). \quad (35)$$

Similarly to (7), the spiking output of the $(N+3)$ -neuron network is given by, for all $t \in \mathbb{R}_{\geq 0}$,

$$u(t) = \sum_{i=0}^{N+2} u_i(t). \quad (36)$$

Note that the two-neuron network in (2)-(7) is a special case of the one in (33)-(36). Indeed, (2)-(7) corresponds to (33)-(36) with $N = 1$, $b_1 = 0$, $c = 0$ (thus the last two neurons in (34) are not needed) and neurons ξ_0 , ξ_1 correspond to neurons ξ_2 and ξ_1 in (2)-(7), respectively. Moreover, since the input to the neuron is a Lebesgue measurable and locally essentially bounded signal and the neuron dynamics in (33) is the same as in (2), Proposition 1 holds *mutatis mutandi* for each neuron of the network. Consequently, since the number of neurons is finite (equal to $N+3$), the spiking signal u in (36) is such that no accumulation of spiking times can happen.

The next theorem, whose proof is given in Appendix D, provides conditions on the neuron parameters $\tilde{\alpha}_i$, $\tilde{\Delta}_i$ and on the gains G_i , $i \in \{0, 1, \dots, N\}$ of the integrate-and-fire neuronal network in Fig. 3 with neurons dynamics in (33) to ensure that the spiking output of the network u in (36) approximates the given PWA function g as defined in (32).

Theorem 4. Consider g in (32). Define $\bar{K}_i := K_i$ for $i \in \{0, 1\}$ and $\bar{K}_i := K_i - K_{i-1}$ for $i \in \{2, 3, \dots, N\}$. For any

$\overline{K}_i, i \in \{0, 1, \dots, N\}$, select $\alpha_i, \Delta_i \in \mathbb{R}_{\geq 0}$ such that $|\overline{K}_i| := \frac{\alpha_i}{\Delta_i}, i \in \{0, 1, \dots, N\}$ and $\mathcal{G}_0 := -\text{sign}(\overline{K}_0), \mathcal{G}_i := \text{sign}(\overline{K}_i), i \in \{1, 2, \dots, N\}$. Moreover, select $\alpha_{N+1} = \Delta_{N+1} \in \mathbb{R}_{>0}$ and $\alpha_{N+2} = \Delta_{N+2} \in \mathbb{R}_{>0}$. Design the $(N+3)$ -neuron integrate-and-fire spiking neuronal network in (33)-(36) with parameters $c, b_i, i \in \{1, 2, \dots, N\}$ from (32) and parameters $\alpha_i, \Delta_i, \mathcal{G}_i, i \in \{0, 1, \dots, N\}$ defined above. Then, for any $y \in \mathcal{L}_{\mathbb{R}}$, for all $t \in \mathbb{R}_{\geq 0}$,

$$\left| \int_0^t g(y(s)) - u(s) ds \right| \leq \sum_{i=0}^{N+2} \alpha_i, \quad (37)$$

with u defined in (36) output of the network.

Theorem 4 proves that, given any PWA function in (32), it is possible to design a SNN of integrate-and-fire neurons which approximates that function in the sense of (37), where the neuron parameters and the network parameters (bias b_i and gains \mathcal{G}_i) depend on the function parameters. Moreover, Theorem 4 shows how these parameters are linked and thus, the result of this theorem also ensures that the spiking output of any given integrate-and-fire SNN with $N+3$ neurons, like the one in (33)-(36) and shown in Fig. 3, approximates a PWA function, whose parameters depends on the neurons' parameters. Note that, similarly to Theorem 1, the bound in (37) can be made arbitrarily small by selecting $\alpha_i, i \in \{0, 1, \dots, N+2\}$ arbitrarily small. This implies Δ_i small, which typically leads to more frequent spikes.

Remark 7. Using the neurons' dynamics and network structure proposed in this section to emulate PWA functions it is possible that several neurons are active, i.e., integrating their input and generating spikes, simultaneously. Indeed, when, for instance $b_i \leq y \leq b_{i+1}$, for some $i \in \{1, 2, \dots, N-1\}$, neurons $\tilde{\xi}_1, \tilde{\xi}_2, \dots, \tilde{\xi}_i$ are all active and one among $\tilde{\xi}_{N+1}$ and $\tilde{\xi}_{N+2}$ is active. Thus, it could happen that, in case the spikes generated by these neurons have opposite sign, they compensate each other. Therefore this might not be the most efficient network design to approximate PWA functions using spiking signals, but this is also not the purpose of this paper. Here we aim to formally show how PWA maps can be emulated through integrate-and-fire SNNs with approximation guarantees. Future work will be related to building more efficient SNN implementations.

IX. NUMERICAL CASE STUDY

We now consider a linearized model of an unstable batch reactor process [43]. This system is given by (1) with matrices

$$A = \begin{bmatrix} 1.38 & -0.2077 & 6.715 & -5.676 \\ -0.5814 & -4.29 & 0 & 0.675 \\ 1.067 & 4.273 & -6.654 & 5.893 \\ 0.048 & 4.273 & 1.343 & -2.104 \end{bmatrix},$$

$$B = \begin{bmatrix} 0 & 0 \\ 5.679 & 0 \\ 1.136 & -3.146 \\ 1.136 & 0 \end{bmatrix}, \quad C = \begin{bmatrix} 1 & 0 & 1 & -1 \\ 0 & 1 & 0 & 0 \end{bmatrix}. \quad (38)$$

The eigenvalues of the open-loop system are $1.99, 0.064, -5.057, -8.67$. It can be verified that this

MIMO system can be stabilized using the static output feedback gain

$$K = \begin{bmatrix} -0.5 & -2 \\ 5 & 0.5 \end{bmatrix}, \quad (39)$$

which results in the closed-loop eigenvalues $-1.519, -2.5, -19.9, -14.84$ and thus renders the closed-loop system asymptotically stable, i.e., $A+BKC$ Hurwitz. Thus, Assumption 1 is satisfied. We emulate this static gain using the spiking controller described in Sections III, IV, and VIII-A. Although we can, in principle, select $\alpha_{1,i,j} \neq \alpha_{2,i,j}$, we set $\alpha_{1,i,j} = \alpha_{2,i,j}$ for all $i \in \{1, 2\}$ and $j \in \{1, 2\}$ to retain symmetry, and we consider three choices for the neuron parameters. For the first spiky controller, we select the amplitudes $\alpha_{i,j}^I := \alpha_{1,i,j}^I = \alpha_{2,i,j}^I$ as

$$[\alpha_{i,j}^I] = \frac{1}{25} \cdot \begin{bmatrix} 1 & 4 \\ 3 & 0.3 \end{bmatrix}. \quad (40)$$

In order to emulate the closed-loop system given by $A+BKC$, we thus set the threshold $\Delta_{i,j}^I := \Delta_{1,i,j}^I = \Delta_{2,i,j}^I$ such that $K_{i,j} = \alpha_{i,j}^I / \Delta_{i,j}^I$, i.e., we take $\Delta_{i,j}^I = \alpha_{i,j}^I / K_{i,j}$ for all $i \in \{1, 2, \dots, n_u\}$ and $j \in \{1, 2, \dots, n_y\}$. To illustrate the emulation property, we also design a second controller with $\alpha_{i,j}^{II} = \frac{1}{4} \alpha_{i,j}^I$ and $\Delta_{i,j}^{II} = \frac{1}{4} \Delta_{i,j}^I$, and a third controller with $\alpha_{i,j}^{III} = \frac{1}{15} \alpha_{i,j}^I$ and $\Delta_{i,j}^{III} = \frac{1}{15} \Delta_{i,j}^I$. Fig. 4 shows the output trajectories of the three spiky controllers based on integrate-and-fire SNNs and the emulated continuous-time SOF controller solution to (8) for initial state $x(0) = \bar{x}(0) = [5.51, 7.08, 2.91, 5.11]^\top$ and $\xi_{\ell,i,j}(0) = 0$ for all $\ell \in \{1, 2\}$, $i \in \{1, 2\}$ and $j \in \{1, 2\}$.

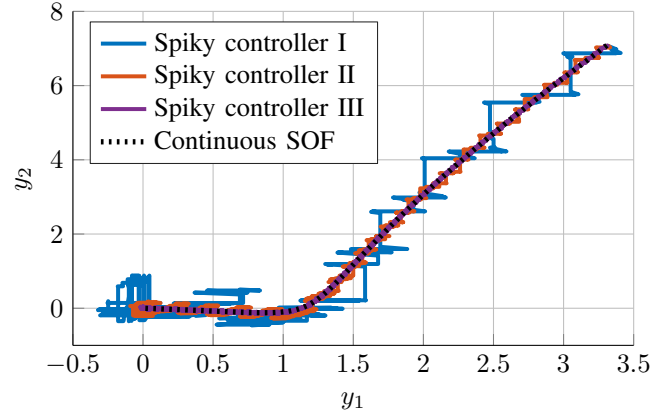


Fig. 4. Emulation of static output-feedback using spiky controllers for a linearized batch reactor.

A number of observations can be made. Firstly, the trajectories in the three cases resemble the closed-loop trajectory of $\dot{\bar{x}} = (A+BKC)\bar{x}$. Secondly, the bound on the state emulation error \tilde{x} from Theorem 3, which corresponds to the ultimate bound of the practical stability property from Corollary 1, becomes smaller when both the threshold and the spike amplitude shrink (retaining their ratio, in order to emulate the same static output feedback gain, see Theorem 1, as expected). Lastly, taking smaller threshold and spike amplitude comes at the cost of more spikes, as we can see in Table I. In fact, the values of the bound on $|\tilde{x}(t)|$ for all $t \in \mathbb{R}_{\geq 0}$ in Theorem 3,

which correspond to the ultimate bound $\limsup_{t \rightarrow \infty} |x(t)|$ in Corollary 1 are also given in Table I computed based on the theoretical guarantees and from the simulations. The simulated values of the norm of the state emulation error $|\tilde{x}(t)|$ are within the guaranteed bounds of Theorem 3. Clearly there is a trade-off between the number of spikes and the ultimate bound and the overall approximation error with respect to $\tilde{x} = (A + BKC)\bar{x}$.

TABLE I

NUMBER OF SPIKES FOR A 10 SECOND SIMULATION AND (THEORETICALLY GUARANTEED AND SIMULATED) BOUND ON $|\tilde{x}(t)|$ FOR ALL $t \geq 0$ OF THE LINEARIZED UNSTABLE BATCH REACTOR SYSTEM STABILIZED USING SPIKY CONTROLLERS.

Controller	I	II	III
No. spikes	175	540	1421
Guaranteed bound on $ \tilde{x} $	3.669	0.917	0.245
Simulation bound on $ \tilde{x} $	0.857	0.236	0.052

X. CONCLUSIONS

This paper presented a systematic spiking control design framework for LTI systems, using a two-step emulation-based design approach to ensure a practical closed-loop stability property. The first step of our approach builds on a formal signal-based “spiky” approximation property of integrate-and-fire spiking neural networks (SNNs) (Theorem 1). In the second step, the novel notion of integral spiking-input-to-state stability (iSISS) was defined and we have ensured that a (pre-compensated) LTI system satisfies it (Theorem 2). Combining these two steps we guaranteed that the trajectories of the spiky control loop remain within a tunable distance to the ideal continuous-time closed-loop system, i.e., the state emulation error can be made small (Theorem 3). This result directly implies that a practical stability property of the closed-loop system also holds (Corollary 1). Generalizations to MIMO LTI systems and the approximation of continuous piecewise affine functions were presented as well.

The formal signal-based approximation property of spiky integrate-and-fire neurons and the iSISS notion are instrumental to ensure stability properties when neuromorphic controllers are considered. We therefore believe that the concepts and reasoning have potential to be generalized to broader classes of systems and thus may inspire several future work directions. In particular, it would be interesting to consider different neuronal models, general nonlinear systems and the emulation of nonlinear dynamic controllers. To generalize the results to nonlinear systems, several key challenges need to be addressed. Thereto, it is necessary to define the concept of solution of nonlinear systems with spiking inputs, in the form of Dirac’s impulses, and then we need to develop conditions under which nonlinear systems are iSISS, possibly generalizing the proof of Theorem 2. In addition, in the future we would like to investigate different designs of the network structure of the SNNs and the choice of gain K to improve the efficiency of the neuron-inspired controller in terms of number of spikes (see Remark 5). Moreover, in the current setting, the input of the neurons is a continuous-time signal. A promising future work direction consists in considering neuromorphic

event-based sensors and thus use spiking measurement signals as inputs to the neurons, as in, e.g., [11], [13].

APPENDIX

A. Proof of Proposition 1

As y is a locally essentially bounded signal, for any $T \in \mathbb{R}_{\geq 0}$ there exists $M_T \in \mathbb{R}_{>0}$ such that $|y(t)| \leq M_T$ for almost all $t \in [0, T]$. From (2), we have, for all $\ell \in \{1, 2\}$, and all $s \in (t_{\ell,i}, t_{\ell,i+1})$, $i \in \{1, 2, \dots, j_{\ell}(t)\}$,

$$\frac{d}{ds} \xi(s) = \max\{0, (3 - 2\ell)y(s)\} \leq M_T. \quad (41)$$

Hence, we have, for any $s \in (t_{\ell,i}, t_{\ell,i+1})$,

$$\xi_{\ell}(s) \leq \xi_{\ell}(t_{\ell,i}^+) + M_T(s - t_{\ell,i}). \quad (42)$$

Since, from (5), $\xi_{\ell}(t_{\ell,i}^+) = 0$, for all $i \in \{1, 2, \dots, j_{\ell}(t)\}$, and from (4), $\xi_{\ell}(t_{\ell,i+1}) = \Delta_{\ell}$, (42) implies, for all $i \in \{1, 2, \dots, j_{\ell}(t) - 1\}$, $t \in [0, T]$, $T \in \mathbb{R}_{\geq 0}$,

$$t_{\ell,i+1} - t_{\ell,i} \geq \frac{\Delta_{\ell}}{M_T}. \quad (43)$$

Hence, on any bounded interval $[0, T]$ there cannot be Zeno behavior, which implies either $j_{\ell} < \infty$ or $t_{\ell,j_{\ell}} \rightarrow \infty$ as $j_{\ell} \rightarrow \infty$ for all $\ell \in \{1, 2\}$. Moreover, the number of neuron is finite (equal to 2) and thus, using $\{t_j\}_{j \in \mathbb{Z}_{\geq 0}} = \{t_{1,j_1}\}_{j_1 \in \mathbb{Z}_{\geq 0}} \cup \{t_{2,j_2}\}_{j_2 \in \mathbb{Z}_{\geq 0}}$, from (43) we have that the sequence $\{t_j\}_{j \in \mathbb{Z}_{\geq 0}}$ is such that $j < \infty$ or it satisfies $t_j \rightarrow \infty$ as $j \rightarrow \infty$, which excludes the Zeno phenomenon. This concludes the proof.

B. Proof of Theorem 1

Let all conditions of Theorem 1 hold. Let $\ell \in \{1, 2\}$ and $t \in \mathbb{R}_{\geq 0}$. Using (6) and $(3 - 2\ell)^2 = 1$, we have for $t \in \mathbb{R}_{\geq 0}$,

$$\begin{aligned} & \int_0^t \max\{0, (3 - 2\ell)K_{\ell}y(s)\} - (3 - 2\ell)u_{\ell}(s)ds \\ &= \int_0^t \max\{0, (3 - 2\ell)K_{\ell}y(s)\} - \sum_{i=1}^{+\infty} \alpha_{\ell}\delta(s - t_{\ell,i})ds. \end{aligned} \quad (44)$$

Using (4), from (44) we have

$$\begin{aligned} & \int_0^t \max\{0, (3 - 2\ell)K_{\ell}y(s)\} - (3 - 2\ell)u_{\ell}(s)ds \\ &= \sum_{i=1}^{j_{\ell}(t)} \int_{t_{\ell,i-1}^+}^{t_{\ell,i}^+} \left[\max\{0, (3 - 2\ell)K_{\ell}y(s)\} - \alpha_{\ell}\delta(s - t_{\ell,i}) \right] ds \\ & \quad + \int_{t_{\ell,j_{\ell}(t)}^+}^t \max\{0, (3 - 2\ell)K_{\ell}y(s)\}ds. \end{aligned} \quad (45)$$

Using $\alpha_{\ell} = K_{\ell}\Delta_{\ell}$, $\ell \in \{1, 2\}$, (45) becomes

$$\begin{aligned} & \int_0^t \max\{0, (3 - 2\ell)K_{\ell}y(s)\} - (3 - 2\ell)u_{\ell}(s)ds \\ &= K_{\ell} \left(\sum_{i=1}^{j_{\ell}(t)} \int_{t_{\ell,i-1}^+}^{t_{\ell,i}^+} \left[\max\{0, (3 - 2\ell)y(s)\} - \Delta_{\ell}\delta(s - t_{\ell,i}) \right] ds \right) \end{aligned}$$

$$+ \int_{t_{\ell, j_\ell(t)}^+}^t \max \{0, (3-2\ell)y(s)\} ds \Big). \quad (46)$$

Moreover, from (2), (5), we have that for all $i \in \{1, 2, \dots, j_\ell(t)\}$ and all $\tilde{t} \in [t_{\ell, i-1}, t_{\ell, i}]$,

$$\xi_\ell(\tilde{t}) = \xi_\ell(t_{\ell, i-1}^+) + \int_{t_{\ell, i-1}^+}^{\tilde{t}} \max \{0, (3-2\ell)y(s)\} ds. \quad (47)$$

Note that, in the interval $[t_{\ell, i-1}, t_{\ell, i}]$ spikes triggered by $\xi_{3-\ell}$ can occur. However, (5) implies that ξ_ℓ will not change when a spike is triggered by $\xi_{3-\ell}$ and thus, (47) holds for all $\tilde{t} \in [t_{\ell, i-1}, t_{\ell, i}]$, $i \in \{1, 2, \dots, j_\ell(t)\}$. Since from (5) we have $\xi_\ell(t_{\ell, i-1}^+) = 0$ for all $i \in \{2, 3, \dots, j_\ell(t)\}$, (47) becomes

$$\xi_\ell(\tilde{t}) = \int_{t_{\ell, i-1}^+}^{\tilde{t}} \max \{0, (3-2\ell)y(s)\} ds \quad (48)$$

Moreover, (4) and (48) imply, for all $i \in \{2, 3, \dots, j_\ell(t)\}$,

$$\Delta_\ell = \xi_\ell(t_{\ell, i}^-) = \int_{t_{\ell, i-1}^+}^{t_{\ell, i}^-} \max \{0, (3-2\ell)y(s)\} ds. \quad (49)$$

Since $y \in \mathcal{L}_{\mathbb{R}}$ we have, for all $\tau \in \mathbb{R}_{\geq 0}$,

$$\int_{\tau^-}^{\tau^+} \max \{0, (3-2\ell)y(s)\} ds = 0. \quad (50)$$

Thus, from (49), and (50) we have, for all $i \in \{2, 3, \dots, j_\ell(t)\}$

$$\Delta_\ell = \int_{t_{\ell, i-1}^+}^{t_{\ell, i}^+} \max \{0, (3-2\ell)y(s)\} ds. \quad (51)$$

From (51) and using the definition of the Dirac delta function, we have for all $i \in \{2, 3, \dots, j_\ell(t)\}$

$$\int_{t_{\ell, i-1}^+}^{t_{\ell, i}^+} \max \{0, (3-2\ell)y(s)\} - \Delta_\ell \delta(s - t_{\ell, i}) ds = 0. \quad (52)$$

Thus, using (52), (46) becomes

$$\begin{aligned} & \int_0^t \max \{0, (3-2\ell)K_\ell y(s)\} - (3-2\ell)u_\ell(s) ds \\ &= K_\ell \left(\int_{t_{\ell, 0}^+}^{t_{\ell, 1}^+} \max \{0, (3-2\ell)y(s)\} - \Delta_\ell \delta(s - t_{\ell, 1}) ds \right. \\ & \quad \left. + \int_{t_{\ell, j_\ell(t)}^+}^t \max \{0, (3-2\ell)y(s)\} ds \right). \end{aligned} \quad (53)$$

From (47) with $i = 1$ and from (48) and (53), we obtain, for all $t \in \mathbb{R}_{\geq 0}$,

$$\begin{aligned} & \int_0^t \max \{0, (3-2\ell)K_\ell y(s)\} - (3-2\ell)u_\ell(s) ds \\ &= K_\ell(-\xi_\ell(0) + \xi_\ell(t)). \end{aligned} \quad (54)$$

Moreover, from (4) and (5) we have that $\xi_\ell(t) \in [0, \Delta_\ell]$ for all $t \in \mathbb{R}_{\geq 0}$. Thus, from (54), using $K_\ell = \frac{\alpha_\ell}{\Delta_\ell}$, we can conclude that, for all $t \in \mathbb{R}_{\geq 0}$, $\ell \in \{1, 2\}$,

$\int_0^t \max \{0, (3-2\ell)K_\ell y(s)\} - (3-2\ell)u_\ell(s) ds \in [-\alpha_\ell, \alpha_\ell]$, which implies,

$$\left| \int_0^t \max \{0, (3-2\ell)K_\ell y(s)\} - (3-2\ell)u_\ell(s) ds \right| \in [0, \alpha_\ell]. \quad (55)$$

This concludes the first part of the proof.

We now prove the second part of Theorem 1. Using $\psi = \max \{0, K_1 y\} - \max \{0, -K_2 y\} - u$, and u from (7) we have

$$\begin{aligned} & \int_0^t \psi(s) ds \\ &= \int_0^t [\max \{0, K_1 y(s)\} - \max \{0, -K_2 y(s)\} - u(s)] ds \\ &= \int_0^t \left[K_1 \max \{0, y(s)\} - \sum_{i=1}^{+\infty} \alpha_1 \delta(s - t_{1,i}) \right] ds - \\ & \quad \int_0^t \left[K_2 \max \{0, -y(s)\} - \sum_{i=1}^{+\infty} -\alpha_2 \delta(s - t_{2,i}) \right] ds. \end{aligned} \quad (56)$$

Using (4), (56) can be rewritten as, following similar steps as in the first part of the proof,

$$\begin{aligned} \int_0^t \psi(s) ds &= \sum_{i=1}^{j_1(t)} \int_{t_{1, i-1}^+}^{t_{1, i}^+} \left[K_1 \max \{0, y(s)\} \right. \\ & \quad \left. - \alpha_1 \delta(s - t_{1,i}) \right] ds + \int_{t_{1, j_1(t)}^+}^t K_1 \max \{0, y(s)\} ds \\ & \quad - \left(\sum_{i=1}^{j_2(t)} \int_{t_{2, i-1}^+}^{t_{2, i}^+} \left[K_2 \max \{0, -y(s)\} - \alpha_2 \delta(s - t_{2,i}) \right] ds \right. \\ & \quad \left. + \int_{t_{2, j_2(t)}^+}^t K_2 \max \{0, -y(s)\} ds \right). \end{aligned} \quad (57)$$

Using $\alpha_\ell = K_\ell \Delta_\ell$, $\ell \in \{1, 2\}$ from (57) we have,

$$\begin{aligned} \int_0^t \psi(s) ds &= K_1 \left(\sum_{i=1}^{j_1(t)} \int_{t_{1, i-1}^+}^{t_{1, i}^+} \left[\max \{0, y(s)\} \right. \right. \\ & \quad \left. \left. - \Delta_1 \delta(s - t_{1,i}) \right] ds + \int_{t_{1, j_1(t)}^+}^t \max \{0, y(s)\} ds \right) \\ & \quad - K_2 \left(\sum_{i=1}^{j_2(t)} \int_{t_{2, i-1}^+}^{t_{2, i}^+} \left[\max \{0, -y(s)\} - \Delta_2 \delta(s - t_{2,i}) \right] ds \right. \\ & \quad \left. + \int_{t_{2, j_2(t)}^+}^t \max \{0, -y(s)\} ds \right). \end{aligned} \quad (58)$$

From (47) and using (52) for $\ell \in \{1, 2\}$, (58) becomes, similarly to (53),

$$\begin{aligned} & \int_0^t \psi(s) ds = K_1 \left(\int_{t_{1, 0}^+}^{t_{1, 1}^+} \max \{0, y(s)\} - \Delta_1 \delta(s - t_{1,1}) ds \right. \\ & \quad \left. + \int_{t_{1, j_1(t)}^+}^t \max \{0, y(s)\} ds \right) - K_2 \left(\int_{t_{2, 0}^+}^{t_{2, 1}^+} \max \{0, -y(s)\} \right. \\ & \quad \left. - \Delta_2 \delta(s - t_{2,1}) ds + \int_{t_{2, j_2(t)}^+}^t \max \{0, -y(s)\} ds \right). \end{aligned} \quad (59)$$

From (47), (48) and (59), similarly to (54), we obtain, for all $t \in \mathbb{R}_{\geq 0}$,

$$\int_0^t \psi(s)ds = K_1(-\xi_1(0) + \xi_1(t)) - K_2(-\xi_2(0) + \xi_2(t)). \quad (60)$$

Moreover, from (4) and (5) we have that $\xi_\ell(t) \in [0, \Delta_\ell]$ for all $t \in \mathbb{R}_{\geq 0}$ and all $\ell \in \{1, 2\}$. Thus, from (60), using $K_\ell = \frac{\alpha_\ell}{\Delta_\ell}$, we can conclude that $-(\alpha_1 + \alpha_2) \leq \int_0^t \psi(s)ds \leq (\alpha_1 + \alpha_2)$, which implies

$$\left| \int_0^t \psi(s)ds \right| \leq \alpha_1 + \alpha_2 \text{ for all } t \in \mathbb{R}_{\geq 0}. \quad (61)$$

Following similar steps as in (60)-(61) and considering the case $\xi_\ell(0) = 0$, $\ell \in \{1, 2\}$, we obtain (12).

C. Proof of Theorem 2

Let all conditions of Theorem 2 hold. By solving the differential equation in (16) with $f(z, v) = Fz + Gv$, and $F \in \mathbb{R}^{n_z \times n_z}$ Hurwitz, we have, for any $z_0 = z(0) \in \mathbb{R}^{n_z}$, for all $t \geq 0$,

$$z(t) = e^{Ft}z_0 + \int_0^t e^{F(t-s)}Gv(s)ds. \quad (62)$$

We introduce the notation $h(\theta) := e^{F\theta}G \in \mathbb{R}^{n_z \times n_v}$, and all $\theta \in \mathbb{R}$, and recalling that $t_0 = 0$ is not a spiking time, the integral term in (62) can be written as

$$\begin{aligned} \int_0^t h(t-s)v(s)ds &= \sum_{i=1}^{j(t)} \left(\int_{t_{i-1}^+}^{t_i^-} h(t-s)v(s)ds \right. \\ &\quad \left. + \int_{t_i^-}^{t_i^+} h(t-s)v(s)ds \right) + \int_{t_{j(t)}^+}^t h(t-s)v(s)ds, \end{aligned} \quad (63)$$

where $j(t) \in \mathbb{Z}_{\geq 0}$ counts the number of spikes up to and including time t and t_i , $i \in \{1, 2, \dots, j(t)\}$, are the spiking times of v , as defined in Definition 1. We now consider the three integrals in (63) separately. We first consider $\int_{t_{i-1}^+}^{t_i^-} h(t-s)v(s)ds$ for all $i \in \{1, 2, \dots, j(t)\}$. Since $h(t-s)$ is continuous for all $t, s \in \mathbb{R}_{\geq 0}$ with $s \leq t$ and v_k is integrable for all $s \in [t_{i-1}^+, t_i^-]$, we can apply the integration by parts [44, Page 64], [45, Page 80] and, recalling that $h(t-t_i) = h(t-t_i^+) = h(t-t_i^-)$ for all $i \in \{1, 2, \dots, j(t)\}$, we obtain

$$\begin{aligned} \int_{t_{i-1}^+}^{t_i^-} h(t-s)v(s)ds &= h(t-t_i) \int_0^{t_i^-} v(\theta)d\theta \\ &\quad - h(t-t_{i-1}) \int_0^{t_{i-1}^+} v(\theta)d\theta \\ &\quad - \int_{t_{i-1}^+}^{t_i^-} \frac{d}{ds}(h(t-s)) \int_0^s v(\theta)d\theta ds. \end{aligned} \quad (64)$$

Similarly, using the integration by parts the last integral in (63) can be written as,

$$\int_{t_{j(t)}^+}^t h(t-s)v(s)ds$$

$$\begin{aligned} &= h(0) \int_0^t v(\theta)d\theta - h(t-t_{j(t)}) \int_0^{t_{j(t)}^+} v(\theta)d\theta \\ &\quad - \int_{t_{j(t)}^+}^t \frac{d}{ds}(h(t-s)) \int_0^s v(\theta)d\theta ds. \end{aligned} \quad (65)$$

We now consider the second term on the right-hand side of (63) and, using the structure of $v = v_1 + v_2$, where $v_1 \in \mathcal{L}_{\mathbb{R}^{n_v}}$, and $v_2(t) := \sum_{i=1}^{\infty} \Theta_i \delta(t-t_i)$ with $t \in \mathbb{R}_{\geq 0}$, we have

$$\begin{aligned} \int_{t_i^-}^{t_i^+} h(t-s)v(s)ds &= \int_{t_i^-}^{t_i^+} h(t-s)v_1(s)ds \\ &\quad + \int_{t_i^-}^{t_i^+} h(t-s)\Theta_i \delta(s-t_i)ds. \end{aligned} \quad (66)$$

Since v_1 is locally essentially bounded, it is locally integrable and thus we have for all $i \in \{1, 2, \dots, j(t)\}$,

$$\int_{t_i^-}^{t_i^+} h(t-s)v_1(s)ds = 0. \quad (67)$$

Moreover, using the definition of the Dirac delta function, (66) becomes, for all $i \in \{1, 2, \dots, j(t)\}$,

$$\int_{t_i^-}^{t_i^+} h(t-s)v(s)ds = h(t-t_i)\Theta_i. \quad (68)$$

From (63), (64), (65) and (68), we obtain

$$\begin{aligned} \int_0^t h(t-s)v(s)ds &= \sum_{i=1}^{j(t)} \left(h(t-t_i) \int_0^{t_i^-} v(\theta)d\theta - h(t-t_{i-1}) \times \right. \\ &\quad \left. \int_{t_{i-1}^+}^{t_i^+} v(\theta)d\theta - \int_{t_{i-1}^+}^{t_i^-} \frac{d}{ds}(h(t-s)) \int_0^s v(\theta)d\theta ds \right. \\ &\quad \left. + h(t-t_i)\Theta_i \right) + h(0) \int_0^t v(\theta)d\theta - h(t-t_{j(t)}) \times \\ &\quad \left. \int_{t_{j(t)}^+}^{t_{j(t)}^+} v(\theta)d\theta - \int_{t_{j(t)}^+}^t \frac{d}{ds}(h(t-s)) \int_0^s v(\theta)d\theta ds. \right) \end{aligned} \quad (69)$$

In view of the structure of v , we have $\int_{t_i^-}^{t_i^+} \frac{d}{ds}(h(t-s)) \int_0^s v(\theta)d\theta ds = 0$, for all $i \in \{1, 2, \dots, j(t)\}$ and thus, by adding $\sum_{i=1}^{j(t)} \int_{t_i^-}^{t_i^+} \frac{d}{ds}(h(t-s)) \int_0^s v(\theta)d\theta ds = 0$, we have that

$$\begin{aligned} \sum_{i=1}^{j(t)} \int_{t_{i-1}^+}^{t_i^-} \frac{d}{ds}(h(t-s)) \int_0^s v(\theta)d\theta ds &+ \int_{t_{j(t)}^+}^t \frac{d}{ds}(h(t-s)) \int_0^s v(\theta)d\theta ds \\ &= \int_0^t \frac{d}{ds}(h(t-s)) \int_0^s v(\theta)d\theta ds. \end{aligned} \quad (70)$$

Consequently, (69) becomes

$$\int_0^t h(t-s)v(s)ds$$

$$\begin{aligned}
&= h(0) \int_0^t v(\theta) d\theta - \int_0^t \frac{d}{ds} (h(t-s)) \int_0^s v(\theta) d\theta ds \\
&\quad + \sum_{i=1}^{j(t)} \left(h(t-t_i) \int_0^{t_i^-} v(\theta) d\theta - h(t-t_{i-1}) \times \right. \\
&\quad \left. \int_0^{t_{i-1}^+} v(\theta) d\theta + h(t-t_i) \Theta_i \right) - h(t-t_{j(t)}) \int_0^{t_{j(t)}^+} v(\theta) d\theta \\
&= h(0) \int_0^t v(\theta) d\theta - \int_0^t \frac{d}{ds} (h(t-s)) \int_0^s v(\theta) d\theta ds \\
&\quad - h(t-t_0) \int_0^{t_0^+} v(\theta) d\theta + \sum_{i=1}^{j(t)} h(t-t_i) \times \\
&\quad \left(\int_0^{t_i^-} v(\theta) d\theta - \int_0^{t_i^+} v(\theta) d\theta + \Theta_i \right) \\
&= h(0) \int_0^t v(\theta) d\theta - \int_0^t \frac{d}{ds} (h(t-s)) \int_0^s v(\theta) d\theta ds \\
&\quad - h(t-t_0) \int_0^{t_0^+} v(\theta) d\theta \\
&\quad + \sum_{i=1}^{j(t)} h(t-t_i) \left(- \int_{t_i^-}^{t_i^+} v(\theta) d\theta + \Theta_i \right). \quad (71)
\end{aligned}$$

Since $v \in \mathcal{S}$ and $t_0 = 0$ is not a spiking time, $h(t-t_0) \int_0^{t_0^+} v(\theta) d\theta = 0$. Thus, from (71), using the definitions of v and of the Dirac delta function, we have

$$\begin{aligned}
&\int_0^t h(t-s)v(s)ds \\
&= h(0) \int_0^t v(\theta) d\theta - \int_0^t \frac{d}{ds} (h(t-s)) \int_0^s v(\theta) d\theta ds \\
&\quad + \sum_{i=1}^{j(t)} h(t-t_i) \left(- \int_{t_i^-}^{t_i^+} v_1(\theta) d\theta \right. \\
&\quad \left. - \int_{t_i^-}^{t_i^+} \Theta_i \delta(\theta-t_i) d\theta + \Theta_i \right) \\
&= h(0) \int_0^t v(\theta) d\theta - \int_0^t \frac{d}{ds} (h(t-s)) \int_0^s v(\theta) d\theta ds \\
&\quad + \sum_{i=1}^{j(t)} h(t-t_i) \left(- \int_{t_i^-}^{t_i^+} v_1(\theta) d\theta + \Theta_i - \Theta_i \right) \\
&= h(0) \int_0^t v(\theta) d\theta - \int_0^t \frac{d}{ds} (h(t-s)) \int_0^s v(\theta) d\theta ds \\
&\quad + \sum_{i=1}^{j(t)} h(t-t_i) \left(- \int_{t_i^-}^{t_i^+} v_1(\theta) d\theta \right). \quad (72)
\end{aligned}$$

Since v_1 is integrable, (67) holds, and thus (72) becomes

$$\begin{aligned}
\int_0^t h(t-s)v(s)ds &= h(0) \int_0^t v(\theta) d\theta \\
&\quad - \int_0^t \frac{d}{ds} (h(t-s)) \int_0^s v(\theta) d\theta ds. \quad (73)
\end{aligned}$$

Consequently, from (62), recalling $h(t-s) = e^{F(t-s)}G \in \mathbb{R}^{n_z \times n_v}$, for all $t, s \in \mathbb{R}$. and using (73) we have, for all

$$\begin{aligned}
t &\geq 0, \\
z(t) &= e^{Ft}z_0 + \int_0^t e^{F(t-s)}Gv(s)ds \\
&= e^{Ft}z_0 + \left(h(0) \int_0^t v(\theta) d\theta - \int_0^t \frac{d}{ds} (h(t-s)) \times \right. \\
&\quad \left. \int_0^s v(\theta) d\theta ds \right). \quad (74)
\end{aligned}$$

Using the definition of $h(t-s)$, we have $h(0) = G$ and $\frac{d}{ds} (h(t-s)) = -Fe^{F(t-s)}G \in \mathbb{R}^{n_z \times n_v}$ for all $t, s \in \mathbb{R}_{\geq 0}$ with $s \leq t$, and thus, from (74), we obtain, for all $t \geq 0$,

$$z(t) = e^{Ft}z_0 + G \int_0^t v(\theta) d\theta + \int_0^t Fe^{F(t-s)}G \int_0^s v(\theta) d\theta ds. \quad (75)$$

From (75) and using the triangular inequality we have, for all $t \in \mathbb{R}_{\geq 0}$,

$$\begin{aligned}
|z(t)| &= \left| e^{Ft}z_0 + G \int_0^t v(\theta) d\theta + \int_0^t Fe^{F(t-s)}G \int_0^s v(\theta) d\theta ds \right| \\
&\leq |e^{Ft}z_0| + \left| G \int_0^t v(\theta) d\theta \right| + \left| \int_0^t Fe^{F(t-s)}G \int_0^s v(\theta) d\theta ds \right| \\
&\leq |e^{Ft}z_0| + \|G\| \|v\|_* + \int_0^t \|Fe^{F(t-s)}G\| \left| \int_0^s v(\theta) d\theta \right| ds \\
&\leq |e^{Ft}z_0| + \|G\| \|v\|_* + \int_0^t \|Fe^{F(t-s)}G\| \|v\|_* ds \\
&\leq |e^{Ft}z_0| + \|G\| \|v\|_* + \int_0^\infty \|Fe^{Fs}G\| ds \|v\|_*. \quad (76)
\end{aligned}$$

Since F is Hurwitz, we have that there exist $c, \lambda \in \mathbb{R}_{>0}$ such that $|e^{Ft}z_0| \leq ce^{-\lambda t}|z_0|$. Thus, (76) becomes

$$|z(t)| \leq ce^{-\lambda t}|z_0| + \left(\|G\| + \int_0^\infty \|Fe^{Fs}G\| ds \right) \|v\|_* = \beta(|z_0|, t) + \gamma \|v\|_*, \quad (77)$$

where $\beta(s, t) = ce^{-\lambda t}s$, $s \in \mathbb{R}_{\geq 0}$ and thus $\beta \in \mathcal{KL}$ and $\gamma = \|G\| + \int_0^\infty \|Fe^{Fs}G\| ds \in \mathbb{R}_{\geq 0}$. Note that $\int_0^\infty \|Fe^{Fs}G\| ds$ is finite because F is Hurwitz. Equation (77) implies that system (16) with $f(z, v) = Fz + Gv$, with $F \in \mathbb{R}^{n_z \times n_z}$ Hurwitz, is iSISS with respect v according to Definition 2.

D. Proof of Theorem 4

Let all conditions of Theorem 4 hold and let $y \in \mathcal{L}_{\mathbb{R}}$. Using $\bar{K}_i = K_i$ for $i \in \{0, 1\}$ and $\bar{K}_i = K_i - K_{i-1}$ for $i \in \{2, 3, \dots, N\}$ and defining $\tilde{y}_i := y - b_i \in \mathbb{R}$, $i \in \{1, 2, \dots, N\}$, the function g in (32) can be written as

$$\begin{aligned}
g(y) &= c - K_0 \max \{0, -(y - b_1)\} + K_1 \max \{0, y - b_1\} \\
&\quad + \sum_{i=2}^N (K_i - K_{i-1}) \max \{0, y - b_i\} \\
&= c - \bar{K}_0 \max \{0, -\tilde{y}_1\} + \sum_{i=1}^N \bar{K}_i \max \{0, \tilde{y}_i\}. \quad (78)
\end{aligned}$$

Using $\mathcal{G}_0 = -\text{sign}(\bar{K}_0)$, $\mathcal{G}_i = \text{sign}(\bar{K}_i)$, $i \in \{1, 2, \dots, N\}$, noting that \bar{K}_i is defined such that the conditions in Theorem 1 hold for each $i \in \{0, 1, \dots, N\}$, and using the fact that \tilde{y}_i is the signal input to neuron ξ_i from (33), by applying (10) for each neuron ξ_i , $i \in \{0, 1, \dots, N\}$, we have, for $i = 0$,

$$\int_0^t \max \{0, -K_0 \tilde{y}_1(s)\} - \mathcal{G}_0 u_0(s) ds \in [-\alpha_0, \alpha_0], \quad (79)$$

and, for each $i \in \{1, 2, \dots, N\}$,

$$\int_0^t \max \{0, K_i \tilde{y}_i(s)\} - \mathcal{G}_i u_i(s) ds \in [-\alpha_i, \alpha_i], \quad (80)$$

with u_i , $i \in \{0, 1, \dots, N\}$, defined in (35). On the other hand, neurons ξ_{N+1} and ξ_{N+2} have input c and $-c$, respectively. Since $c \in \mathbb{R}$ is a constant, only one of them generates spikes. Moreover, using $\alpha_{N+1} = \Delta_{N+1} \in \mathbb{R}_{>0}$ and $\alpha_{N+2} = \Delta_{N+2} \in \mathbb{R}_{>0}$, we have $K_{N+1} = K_{N+2} = 1 = \frac{\alpha_{N+1}}{\Delta_{N+1}} = \frac{\alpha_{N+2}}{\Delta_{N+2}}$. Recalling $\mathcal{G}_{N+1} = 1$, $\mathcal{G}_{N+2} = -1$, using (10) we have

$$\begin{aligned} \int_0^t \max \{0, c\} - u_{N+1}(s) ds &\in [-\alpha_{N+1}, \alpha_{N+1}], \\ \int_0^t \max \{0, -c\} - u_{N+2}(s) ds &\in [-\alpha_{N+2}, \alpha_{N+2}], \end{aligned} \quad (81)$$

which implies

$$\begin{aligned} \int_0^t c - (u_{N+1} - u_{N+2})(s) ds \\ \in [-\alpha_{N+1} - \alpha_{N+2}, \alpha_{N+1} + \alpha_{N+2}]. \end{aligned} \quad (82)$$

From (35), (36), (78), (79), (80) and (82), we obtain (37). This concludes the proof.

E. Normed space of spiking signals

The iSISS property we have defined in Section VI uses the space \mathcal{S}^{n_v} of spiking signals equipped with $\|v\|_* = \sup_{t \in \mathbb{R}_{\geq 0}} |\int_0^t v(s) ds|$, see Definition 1. In this subsection, we prove that this results in a normed space.

Lemma 1. *The space \mathcal{S}^{n_v} equipped with $\|\cdot\|_*$ as in Definition 1 is a normed space, i.e., \mathcal{S}^{n_v} is a real vector space and, for any $v \in \mathcal{S}^{n_v}$, $\|v\|_* = \sup_{t \in \mathbb{R}_{\geq 0}} |\int_0^t v(s) ds| \in \mathbb{R}_{\geq 0}$ satisfies the axioms of a norm:*

- (i) (Positive definiteness) $\|v\|_* > 0$ for all $v \neq 0$ and $\|v\|_* = 0$ if and only if $v = 0$.¹
- (ii) (Homogeneity) $\|av\|_* = |a| \|v\|_*$ for any $a \in \mathbb{R}$.
- (iii) (Triangle inequality) For any $v, w \in \mathcal{S}^{n_v}$, $\|v + w\|_* \leq \|v\|_* + \|w\|_*$.

Proof of item (i). Clearly, we have $\|v\|_* \geq 0$ for all $v \in \mathcal{S}^{n_v}$. Moreover, when $v = 0$ we have $\sup_{t \in \mathbb{R}_{\geq 0}} |\int_0^t v(s) ds| = 0$. On the other hand, $\sup_{t \in \mathbb{R}_{\geq 0}} |\int_0^t v(s) ds| = 0$ implies $|\int_0^t v(s) ds| = |\int_0^t (v_1(s) + v_2(s)) ds| = 0$ for all $t \in \mathbb{R}_{\geq 0}$ and thus $\int_\tau^t v(s) ds = 0$ for all $0 \leq \tau < t$. Since v_2 consists of a sequence of Dirac pulses, its integral on a sufficiently small

¹Note that a spiking signal $v \in \mathcal{S}^{n_v}$, i.e., $v(t) = v_1(t) + v_2(t)$ with $v_1(t) \in \mathcal{L}_{\mathbb{R}^{n_v}}$ and $v_2(t) = \sum_{i=1}^{\infty} \Theta_i \delta(t - t_i)$ as in Definition 1, is zero ($v = 0$), when v_1 is zero in Lebesgue sense and thus $v_1(t) = 0$ for almost all $t \in \mathbb{R}_{\geq 0}$ and $\Theta_i = 0$, $i \in \{1, 2, \dots\}$, and thus $v_2(t) = 0$ for all $t \in \mathbb{R}_{\geq 0}$.

interval $[\tau, t]$ containing a single Dirac time t_i (with $\Theta_i \neq 0$) has to be zero as otherwise $\int_\tau^t v_1(s) ds = -\int_\tau^t v_2(s) ds$ cannot hold because v_1 locally essentially bounded function. Indeed, the right-hand side of this inequality converges to zero when $t - \tau$ approaches zero, while the right-hand side would take the value $\Theta_i \neq 0$, which would be a contradiction and thus $\Theta_i = 0$. Hence, $v_2 = 0$ and thus also $\int_\tau^t v_1(s) ds = 0$ for all $0 \leq \tau < t$. Using the Lebesgue differentiation theorem [46, Theorem 3.21], we have, for almost $t \in \mathbb{R}_{\geq 0}$, $v_1(t) = \lim_{\varepsilon \downarrow 0} \int_{t-\varepsilon}^{t+\varepsilon} v_1(s) ds = v_1(t)$. As we know that the intervals in the limit are all zero, we get that $v_1(t) = 0$ for almost all $t \in \mathbb{R}_{\geq 0}$. Therefore, $\|v\|_* = \sup_{t \in \mathbb{R}_{\geq 0}} |\int_0^t v(s) ds| = 0$ if and only if $v = 0$. This concludes the proof of item (i).

Items (ii) and (iii) follow straightforwardly.

REFERENCES

- [1] C. A. Mead, “Neuromorphic electronic systems,” *Proceedings of the IEEE*, vol. 78, no. 10, pp. 1629–1636, 1990.
- [2] G. Gallego, T. Delbrück, G. Orchard, C. Bartolozzi, B. Taba, A. Censi, S. Leutenegger, A. J. Davison, J. Conradt, K. Daniilidis, and D. Scaramuzza, “Event-based vision: A survey,” *IEEE Transactions on Pattern Analysis and Machine Intelligence*, vol. 44, no. 1, pp. 154–180, 2022.
- [3] I. Krauhausen, D. A. Koutsouras, A. Melianas, S. T. Keene, K. Lieberth, H. Ledanseur, R. Sheelamanthula, A. Giovannitti, F. Torricelli, I. McCulloch, P. W. M. Blom, A. Salleo, Y. van de Burgt, and P. Gkoupidenis, “Organic neuromorphic electronics for sensorimotor integration and learning in robotics,” *Science Advances*, vol. 7, no. 50, p. eabl5068, 2021.
- [4] A. Shrestha, H. Fang, Z. Mei, D. P. Rider, Q. Wu, and Q. Qiu, “A survey on neuromorphic computing: Models and hardware,” *IEEE Circuits and Systems Magazine*, vol. 22, no. 2, pp. 6–35, 2022.
- [5] K. Yamazaki, V.-K. Vo-Ho, D. Bulsara, and N. Le, “Spiking neural networks and their applications: A review,” *Brain sciences*, vol. 12, no. 7, p. 863, 2022.
- [6] P. Singh, S. Z. Yong, and E. Fazzoli, “Regulation of linear systems using event-based detection sensors,” *IEEE Transactions on Automatic Control*, vol. 64, no. 1, pp. 373–380, 2018.
- [7] S. P. DeWeerth, L. Nielsen, C. A. Mead, and K. J. Åström, “A neuron-based pulse servo for motion control,” in *IEEE International Conference on Robotics and Automation*, pp. 1698–1703, 1990.
- [8] S. P. DeWeerth, L. Nielsen, C. A. Mead, and K. J. Åström, “A simple neuron servo,” *IEEE Transactions on Neural Networks*, vol. 2, no. 2, pp. 248–251, 1991.
- [9] L. Ribar and R. Sepulchre, “Neuromorphic control: Designing multiscale mixed-feedback systems,” *IEEE Control Systems Magazine*, vol. 41, no. 6, pp. 34–63, 2021.
- [10] R. Sepulchre, “Spiking control systems,” *Proceedings of the IEEE*, vol. 110, no. 5, pp. 577–589, 2022.
- [11] R. Schmetterling, F. Forni, A. Franci, and R. Sepulchre, “Neuromorphic control of a pendulum,” *IEEE Control Systems Letters*, vol. 8, pp. 1235–1240, 2024.
- [12] E. Petri, R. Postoyan, and W. P. M. H. Heemels, “Rhythmic neuromorphic control of a pendulum: A hybrid systems analysis,” *IEEE Conference on Decision and Control*, Rio de Janeiro, Brazil, 2025.
- [13] T. Medvedeva, A. Franci, and F. Castaños, “Formalizing neuromorphic control systems: A general proposal and a rhythmic case study,” *IEEE Conference on Decision and Control*, Rio de Janeiro, Brazil, 2025.
- [14] P. Feketa, T. Birkben, M. Noll, A. Schaum, T. Meurer, and H. Kohlstedt, “Artificial homeostatic temperature regulation via bio-inspired feedback mechanisms,” *Scientific Reports*, vol. 13, no. 1, p. 5003, 2023.
- [15] J. M. Rosito, E. Petri, E. Steur, and W. P. M. H. Heemels, “Design, modelling and analysis of a bio-inspired spiking temperature regulator,” *IEEE Conference on Decision and Control*, Rio de Janeiro, Brazil, 2025.
- [16] P. Agliati, A. Urbano, P. Lanillos, N. Ahmad, M. van Gerven, and S. Keemink, “Spiking neurons as predictive controllers of linear systems,” *arXiv preprint arXiv:2507.16495*, 2025.
- [17] L. T. C. Jansen, E. Petri, M. van Berkel, and W. P. M. H. Heemels, “Nuclear fusion plasma fuelling with ice pellets using a neuromorphic controller,” *IEEE Conference on Decision and Control*, Rio de Janeiro, Brazil, 2025.

[18] P. J. Antsaklis *et al.*, “Neural networks for control systems,” *IEEE Transactions on Neural Networks*, vol. 1, no. 2, pp. 242–244, 1990.

[19] B. Bavarian, “Introduction to neural networks for intelligent control,” *IEEE Control Systems Magazine*, vol. 8, no. 2, pp. 3–7, 2002.

[20] D. Psaltis, A. Sideris, and A. A. Yamamura, “A multilayered neural network controller,” *IEEE control systems magazine*, vol. 8, no. 2, pp. 17–21, 2002.

[21] E. Petri, K. J. A. Scheres, E. Steur, and W. P. M. H. Heemels, “Analysis of a simple neuromorphic controller for linear systems: A hybrid systems perspective,” *IEEE Conference on Decision and Control*, Milan, Italy, pp. 8578–8583, 2024.

[22] L. Lapicque, “Recherches quantitatives sur l’excitation électrique des nerfs traitée comme une polarization,” *J. Physiol. Pathol. Gen.* 9:620–635, 1907.

[23] L. F. Abbott, “Lapicque’s introduction of the integrate-and-fire model neuron (1907),” *Brain research bulletin*, vol. 50, no. 5-6, pp. 303–304, 1999.

[24] E. M. Izhikevich, “Hybrid spiking models,” *Philosophical Transactions of the Royal Society A: Mathematical, Physical and Engineering Sciences*, vol. 368, no. 1930, pp. 5061–5070, 2010.

[25] W. Gerstner and W. M. Kistler, *Spiking neuron models: Single neurons, populations, plasticity*. Cambridge University Press, 2002.

[26] N. Iannella and A. D. Back, “A spiking neural network architecture for nonlinear function approximation,” *Neural networks*, vol. 14, no. 6-7, pp. 933–939, 2001.

[27] W. Maass, “Fast sigmoidal networks via spiking neurons,” *Neural computation*, vol. 9, no. 2, pp. 279–304, 1997.

[28] E. D. Sontag, “Comments on integral variants of ISS,” *Systems & Control Letters*, vol. 34, no. 1-2, pp. 93–100, 1998.

[29] D. Angeli, E. D. Sontag, and Y. Wang, “A characterization of integral input-to-state stability,” *IEEE Transactions on Automatic Control*, vol. 45, no. 6, pp. 1082–1097, 2000.

[30] E. Petri, K. J. A. Scheres, E. Steur, and W. P. M. H. Heemels, “Spiking control for the stabilization of linear time-invariant systems: an emulation-based design approach,” *IEEE Conference on Decision and Control*, Rio de Janeiro, Brazil, 2025.

[31] A. Astolfi and P. Colaneri, “Static output feedback stabilization: from linear to nonlinear and back,” in *Nonlinear control in the Year 2000*, pp. 49–71, Springer, 2007.

[32] E. Chicca, D. Badoni, V. Dante, M. D’Andreagiovanni, G. Salina, L. Carota, S. Fusi, and P. Del Giudice, “A VLSI recurrent network of integrate-and-fire neurons connected by plastic synapses with long-term memory,” *IEEE Transactions on neural networks*, vol. 14, no. 5, pp. 1297–1307, 2003.

[33] G. Indiveri, E. Chicca, and R. Douglas, “A VLSI array of low-power spiking neurons and bistable synapses with spike-timing dependent plasticity,” *IEEE transactions on neural networks*, vol. 17, no. 1, pp. 211–221, 2006.

[34] J. V. Arthur and K. A. Boahen, “Silicon-neuron design: A dynamical systems approach,” *IEEE Transactions on Circuits and Systems I: Regular Papers*, vol. 58, no. 5, pp. 1034–1043, 2010.

[35] S. Schultz and M. Jabi, “Analogue VLSI ‘integrate-and-fire’ neuron with frequency adaptation,” *Electronics Letters*, vol. 31, no. 16, pp. 1357–1358, 1995.

[36] E. M. Izhikevich, *Dynamical systems in neuroscience*. MIT press, 2007.

[37] Y. van De Burgt, A. Melianas, S. T. Keene, G. Malliaras, and A. Salleo, “Organic electronics for neuromorphic computing,” *Nature Electronics*, vol. 1, no. 7, pp. 386–397, 2018.

[38] W. Wang, A. R. Teel, and D. Nešić, “Analysis for a class of singularly perturbed hybrid systems via averaging,” *Automatica*, vol. 48, no. 6, pp. 1057–1068, 2012.

[39] R. G. Sanfelice and A. R. Teel, “On singular perturbations due to fast actuators in hybrid control systems,” *Automatica*, vol. 47, no. 4, pp. 692–701, 2011.

[40] V. Nair and G. E. Hinton, “Rectified linear units improve restricted boltzmann machines,” in *Proceedings of the 27th international conference on machine learning (ICML-10)*, pp. 807–814, 2010.

[41] P. Ramachandran, B. Zoph, and Q. V. Le, “Searching for activation functions,” *arXiv preprint arXiv:1710.05941*, 2017.

[42] A. Tanwani, B. Brogliato, and C. Prieur, “Stability notions for a class of nonlinear systems with measure controls,” *Mathematics of Control, Signals, and Systems*, vol. 27, pp. 245–275, 2015.

[43] M. Green and D. J. N. Limebeer, *Linear robust control*. Mineola, NY: Dover Publications, 2012.

[44] E. Pap, *Handbook of measure Theory: In two volumes*. Elsevier, 2002.

[45] D. H. Fremlin, *Measure theory, Volume 2: Broad Foundations*. Torres Fremlin, 2000.

[46] G. B. Folland, *Real analysis: modern techniques and their applications*. John Wiley & Sons, 1999.